AOI[3]: Smart Refractory Sensor Systems for Wireless Monitoring of Temperature, Health, and Degradation of Slagging Gasifiers

PI Team:

Dr. Debangsu Bhattacharyya [a]

Mr. Jeffrey Bogan [b]

Dr. David Graham [c]

Dr. Vinod Kulathumani [c]

Dr. Edward M. Sabolsky [d]

[a]Department of Chemical Engineering, WVU

[b]HarbisonWalker International Technology Center

[c]Lane Department of Computer Science and Electrical Engineering, WVU

[d]Department of Mechanical and Aerospace Engineering, WVU

Researcher Team:

- **Post-doc**
  - Rajalekshmi Pillai
- **Graduate Students**
  - **Qiao Huang**
  - Gunes Yakaboylu
  - Steven Andryzcik
  - Priyashraba Misra
- **Undergraduate Students**
  - Brian Armour
  - James Meyer
- **HWI Team**
  - Margaret Raughley
  - Joshua Sayre

Acknowledgements:

- We would like to thank **U.S. Department of Energy (DOE)** for funding the project under contract **DE-FE0012383**.
- **Dr. Maria Reidpath**, U. S. Department of Energy, is greatly appreciated for her insight and valuable guidance.
- We also would like to acknowledge WVU Shared Facilities.
- Thanks to HarbisonWalker International for the technical staff.
- Kindly acknowledge Faculty and staff of West Virginia University for their support.

Background- Gasifier Sensing Needs:

- Online monitoring sensors of refractory used in coal gasifiers under extreme conditions including high temperature (>1300^{o}C) and high pressure (up to 1000 psi) for >20,000 hr.
- Erosive and corrosive conditions (due to slag and high pressure, in addition to various pO_2 levels) causes degradation of refractory over time.
- Ability to monitor the integrity of the refractory materials during gasifier operation would contribute significantly to improving the overall operational performance and reliability of coal gasifiers.
  - Temperature
  - Stress/strain within refractory liner
  - Spallation events
  - Refractory liner health
- Monitoring interior thermochemical conditions allows for efficient control of the gasification process.

Technology Vision:

Item A represents the "smart refractory" material.

Item B is an interconnection (alignment) pin.

Item C is an interconnection brick, which will permit transfer of the signal to the exterior wall.

Item D is the sealed electrical access port to connect to the signal acquisition/processing units.

Item E is low-power electronics and wireless communication.

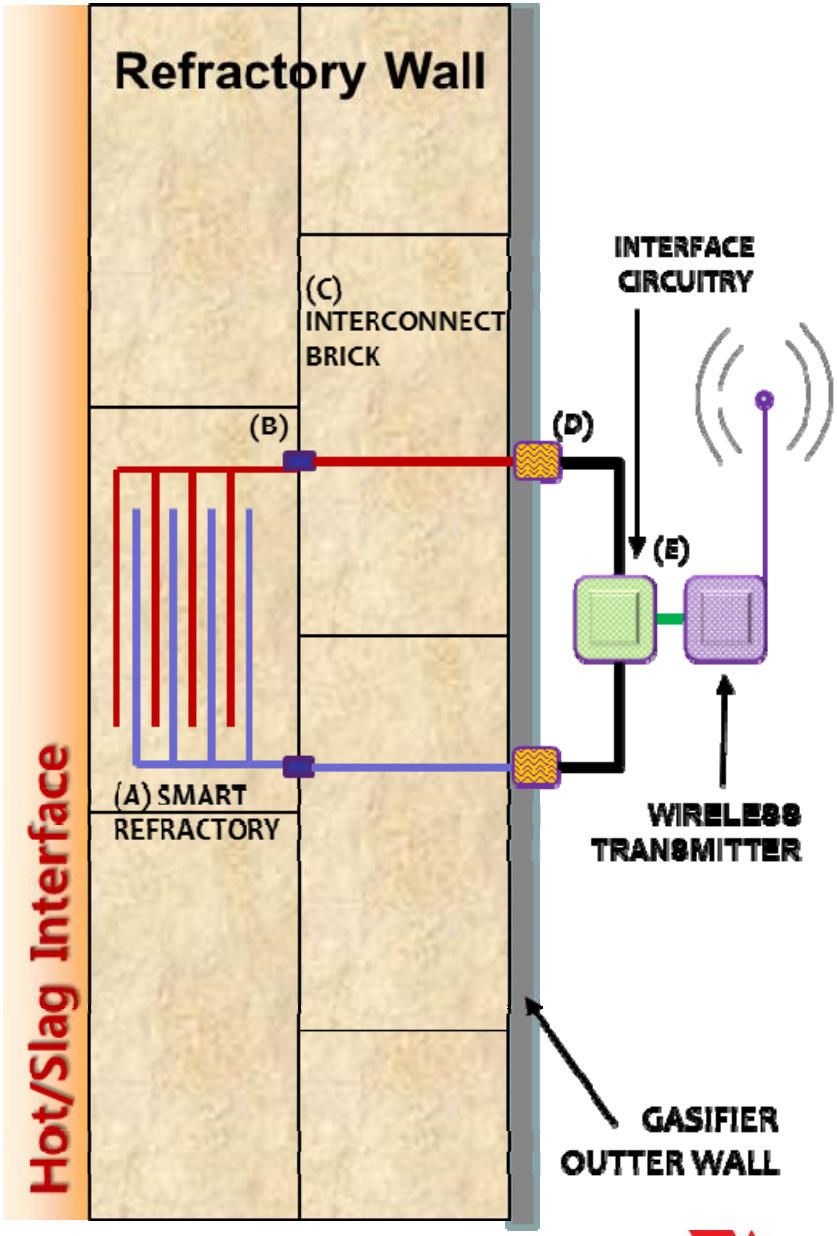

Program Objectives:

1) Investigate chemical stability, thermomechanical properties, and electrical properties of refractory ceramic composites at temperatures between 750-1450ºC.

2) Define processes to pattern and embed the conductive ceramic composites within refractory materials to incorporate temperature and strain/stress sensors into refractory bricks.

3) Develop methods to interface the electrical sensing outputs from the smart refractory with an embedded processor and to design a wireless sensor network to efficiently collect the data at a processing unit for further data analysis.

4) Develop algorithms for model-based estimation of temperature profile in the refractory, slag penetration depth, spallation thickness, and resultant health by using the data from the wireless sensor network.

Task Assignments:

- Task 2: *Fabrication and Characterization of Oxide-Silicide Composites.*
- Task 3 and Task 4: *Sensor Patterning and Embedding and Static and Dynamic Sensor Testing.*
- Task 5: *Data Ex-Filtration Using a Wireless Sensor Network.*
- Task 6: *Model-Based Estimation of Refractory Degradation/Temperature.*

Task 2: Fabrication and Characterization of Oxide-Silicide Composites. (Sabolsky)

Task 2.0 Objectives:

- Investigate chemical stability, thermomechanical properties, and electrical properties of refractory silicide-oxide composites at temperatures between 750-1450°C.

Silicide/Oxide Stability (XRD):

** Prepared via mixed oxide route followed by sintering in Argon atmosphere at 1400°-1600°C.*

	Al_2O_3	Y_2O_3	ZrO_2	Cr_2O_3
$MoSi_2$	$MoSi_2$, Al_2O_3, Mo_5Si_3, SiO_2	$MoSi_2$, Y_2O_3, SiO_2, $Y_5Mo_2O_{12}$, Mo_3Si, Mo_3O	$MoSi_2$, ZrO_2, Mo_5Si_3	$MoSi_2$, Cr_2O_3, Cr_3Mo, SiO_2
WSi_2	WSi_2, Al_2O_3, W_5Si_3	WSi_2, Y_2SiO_5, WO_2, SiO_2	WSi_2, ZrO_2, W_5Si_3	WSi_2, Cr_2O_3, SiO_2, W_3O
$ZrSi_2$	$ZrSi_2$, Al_2O_3, ZrO_2, SiO_2	$ZrSi_2$, Y_2O_3, $Y_2Si_2O_7$, SiO_2	$ZrSi_2$, ZrO_2, SiO_2	$ZrSi_2$, Cr_2O_3, $ZrSiO_4$, Cr_3O, SiO_2
$TaSi_2$	$TaSi_2$, Al_2O_3, Ta_5Si_3, Ta_3Si, SiO_2	$TaSi_2$, Y_2SiO_5, Ta_2O_5, $Y_{10}Ta_4O_{25}$	$TaSi_2$, ZrO_2, Ta_5Si_3, SiO_2	$TaSi_2$, Cr_2O_3, $CrTaO_4$, Ta_2O_5, TaO_2
$NbSi_2$	$NbSi_2$, Al_2O_3, Nb_5Si_3	$NbSi_2$, Y_2O_3, Y_2SiO_5, Nb_5Si_3, SiO_2	$NbSi_2$, ZrO_2, Nb_5Si_3, SiO_2	$NbSi_2$, Cr_2O_3, Nb_5Si_3, $CrNbO_4$, $CrNbSi$, SiO_2
$TiSi_2$	$TiSi_2$, Al_2O_3, Ti_5Si_3, SiO_2	$TiSi_2$, Y_2O_3, $Y_2Si_2O_7$, TiO_2, SiO_2	$TiSi_2$, ZrO_2, TiO_2, SiO_2	$(Cr_{0.88}Ti_{0.12})_2O_3$, Cr_3Si, SiO_2
$CrSi_2$	$CrSi_2$, Al_2O_3, Cr_5Si_3	$CrSi_2$, Y_2O_3, Y_2SiO_5	$CrSi_2$, ZrO_2	$CrSi_2$, Cr_2O_3, Cr_3Si, SiO_2

- Metal silicides show high stability in Al_2O_3 and ZrO_2 matrix only with formation of different type of silicides (Mo_5Si_3, W_5Si_3, Ta_5Si_3, Nb_5Si_3, Cr_5Si_3) and SiO_2 (highlighted).
- They partially react with Y_2O_3 and Cr_2O_3 to form undesired secondary phases.

Silicide/Oxide Microstructure (SEM):

(60-40) vol% $MoSi_2$-Al_2O_3

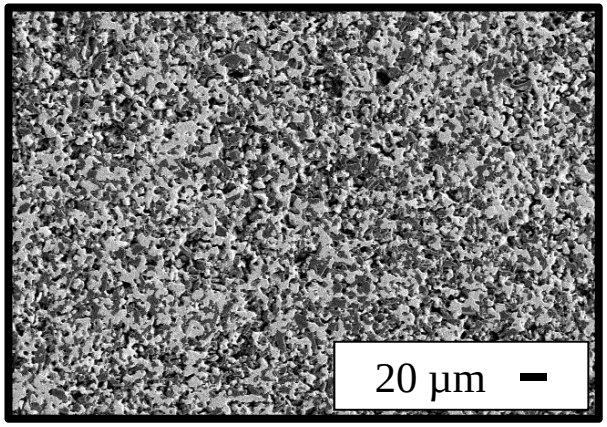

(60-40) vol% $MoSi_2$-Y_2O_3

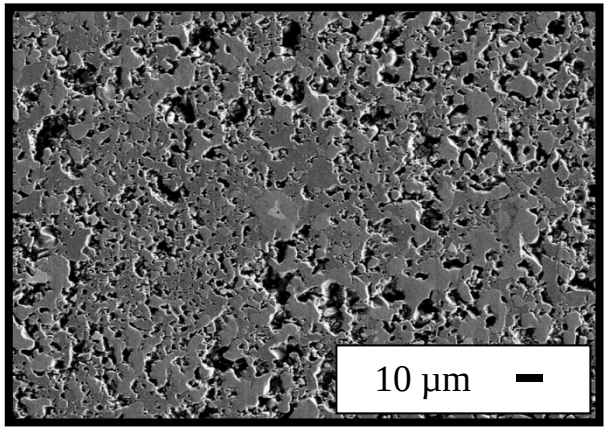

(60-40) vol% $MoSi_2$-ZrO_2

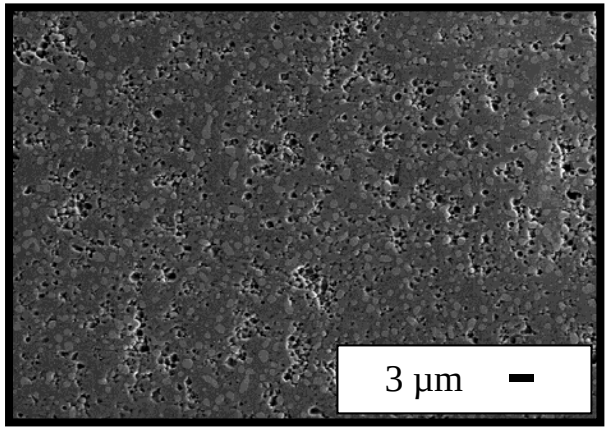

(60-40) vol% WSi_2-Al_2O_3

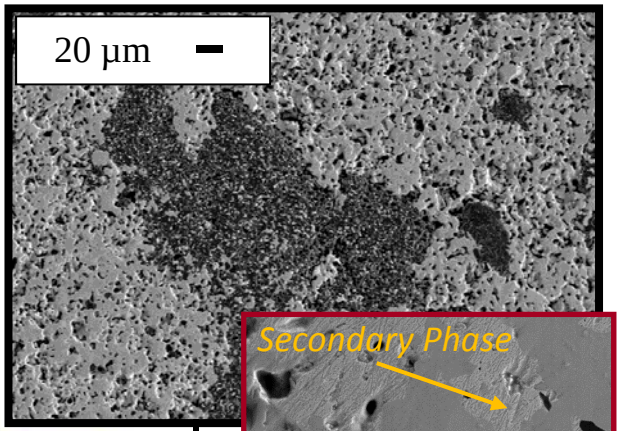

(60-40) vol% WSi_2-Y_2O_3

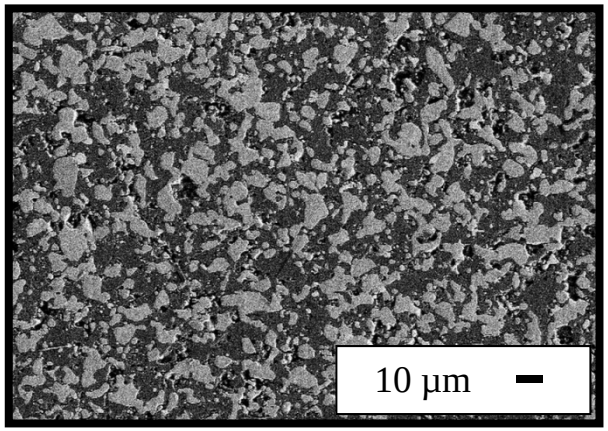

(60-40) vol% WSi_2-ZrO_2

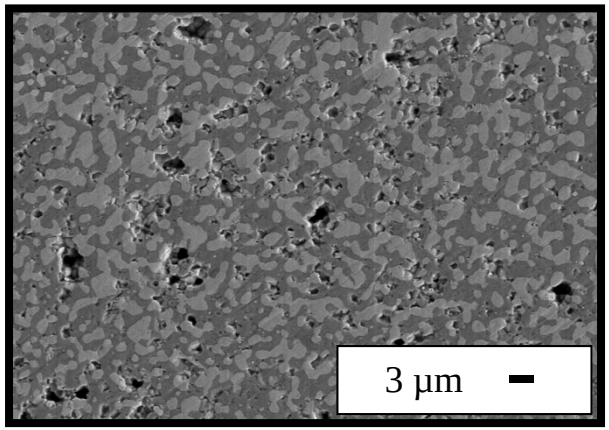

Chemically etched in 1:1:1 $HCl:HNO_3:H_2O$

Silicide/Oxide Properties:

CTE (100°-1000°C)

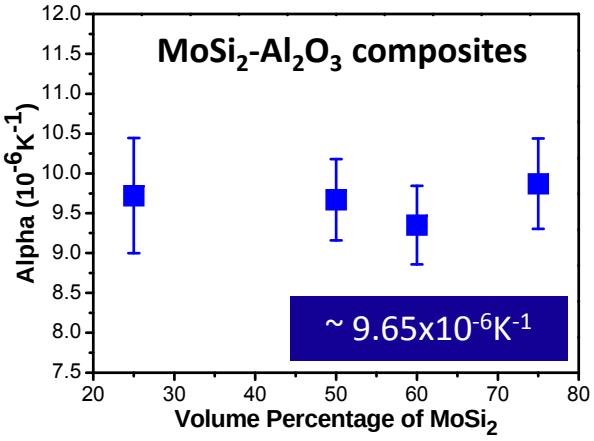

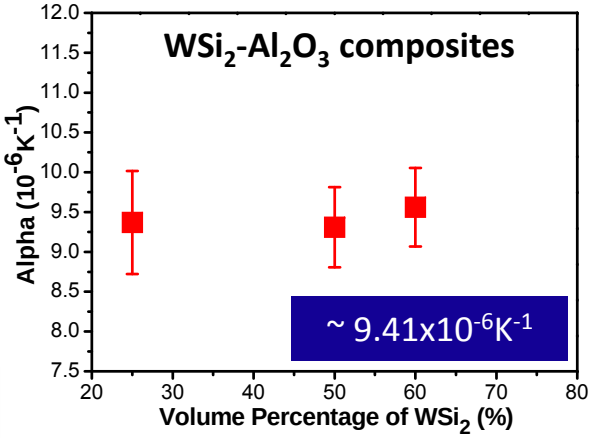

4-point DC Conductivity (100°-1000°C)

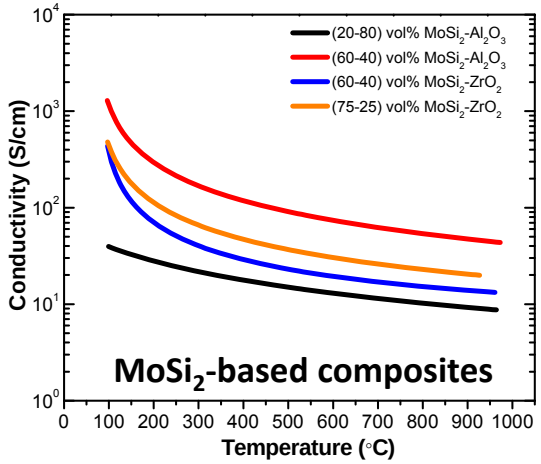

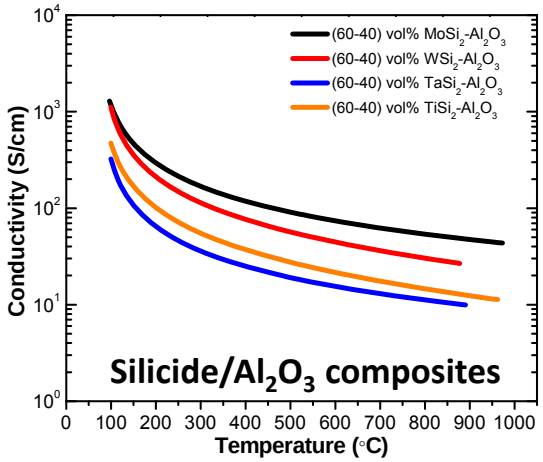

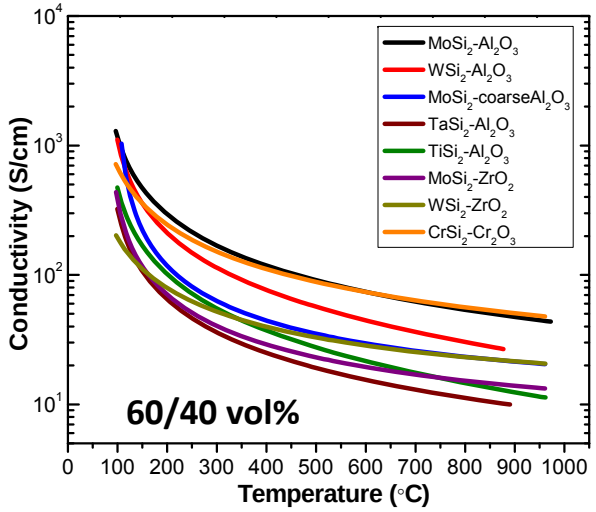

	σ at ~ 1000°C (S/cm)
$MoSi_2$-Al_2O_3	43.6
WSi_2-Al_2O_3	26.7
WSi_2-ZrO_2	20.7
$MoSi_2$-c.Al_2O_3	20.5

- **Key Parameters**: **(1)** metal silicide type and fraction, **(2)** mixedness or level of homogeneity, **(3)** relative density, and **(4)** particle size of the metal silicide and refractory oxide.

Long-Term Stability of the Composites:

Thermal Stability (1400°C)

$MoSi_2$-Al_2O_3 composite

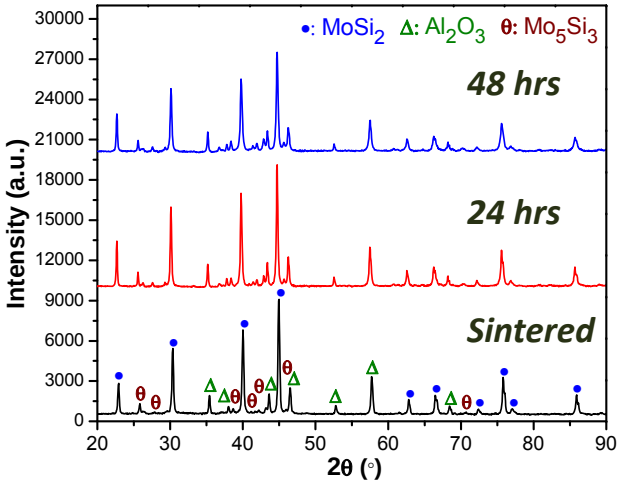

$MoSi_2$-ZrO_2 composite

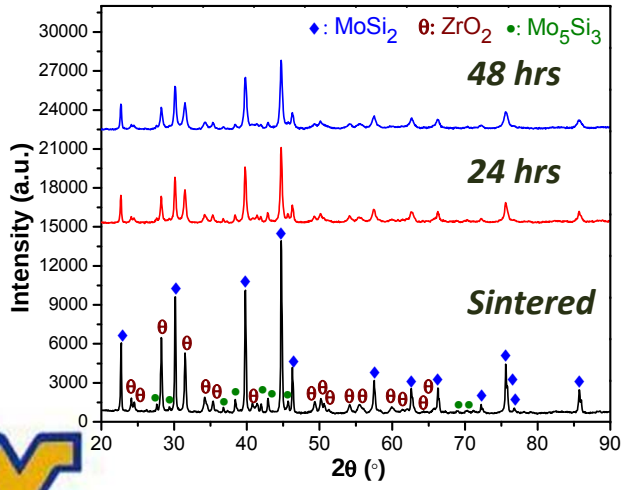

Grain Growth Kinetics (1400°-1600°C)

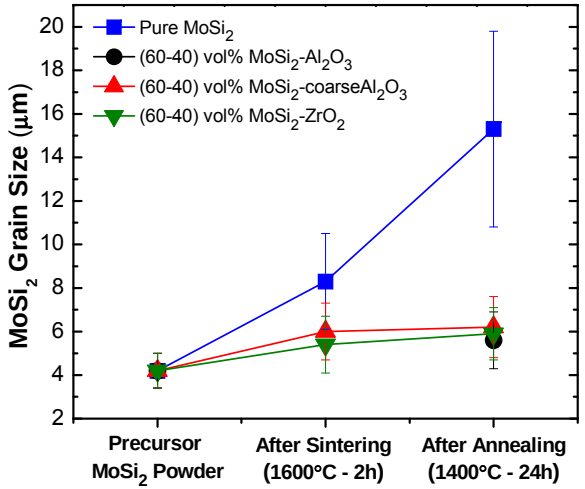

After annealing

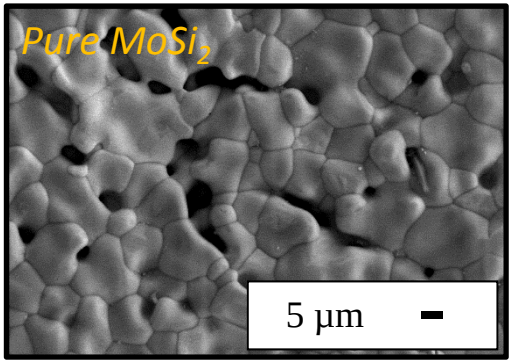

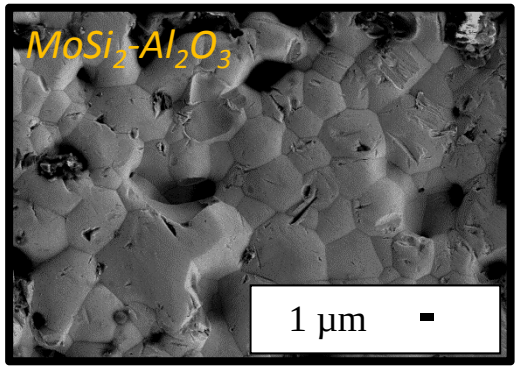

- Silicide/Al_2O_3 and silicide/ZrO_2 composites are highly stable at 1400°C (up to 48 hrs).
- Refractory oxides successfully retard the grain growth.

Task 2 Conclusions and Future Work:

- Metal silicides show high stability in Al_2O_3 and ZrO_2 matrix (with occasional formation of sub-silicides).
- Electrical conductivity of composites characterized with various silicide content→ consistent performance transferred to sensor design and fabrication task.

Future Work:

- Alternative materials and designs (layered structure…) will be investigated to prevent the reaction between silicide/oxide composites and Cr_2O_3.
- Process parameters will be optimized by correlating the degree of distribution (D index) with the physical properties of the composites (conductivity…) at high temperatures.

Task 3: Sensor Patterning and Embedding.(Sabolsky/HWI)

Task 4: Static and Dynamic Sensor Testing of Smart Refractory Specimens. (Sabolsky/HWI)

*US Provisional Patent Number 61/941,159

Task 3 Objectives:

- To develop methods for patterning technology the ceramic composites within the refractory matrix.

Task 4 Objectives:

- To test the electrical performance of the smart refractory brick (with embedded thermocouple or thermistor sensors).
- To investigate corrosion/erosion kinetics in static and dynamic tests on smaller prototype and full-size smart cups and bricks (at WVU and HWI).
- To implement and test methods for data collection on initial prototypes.

Smart Refractory Fabrication:

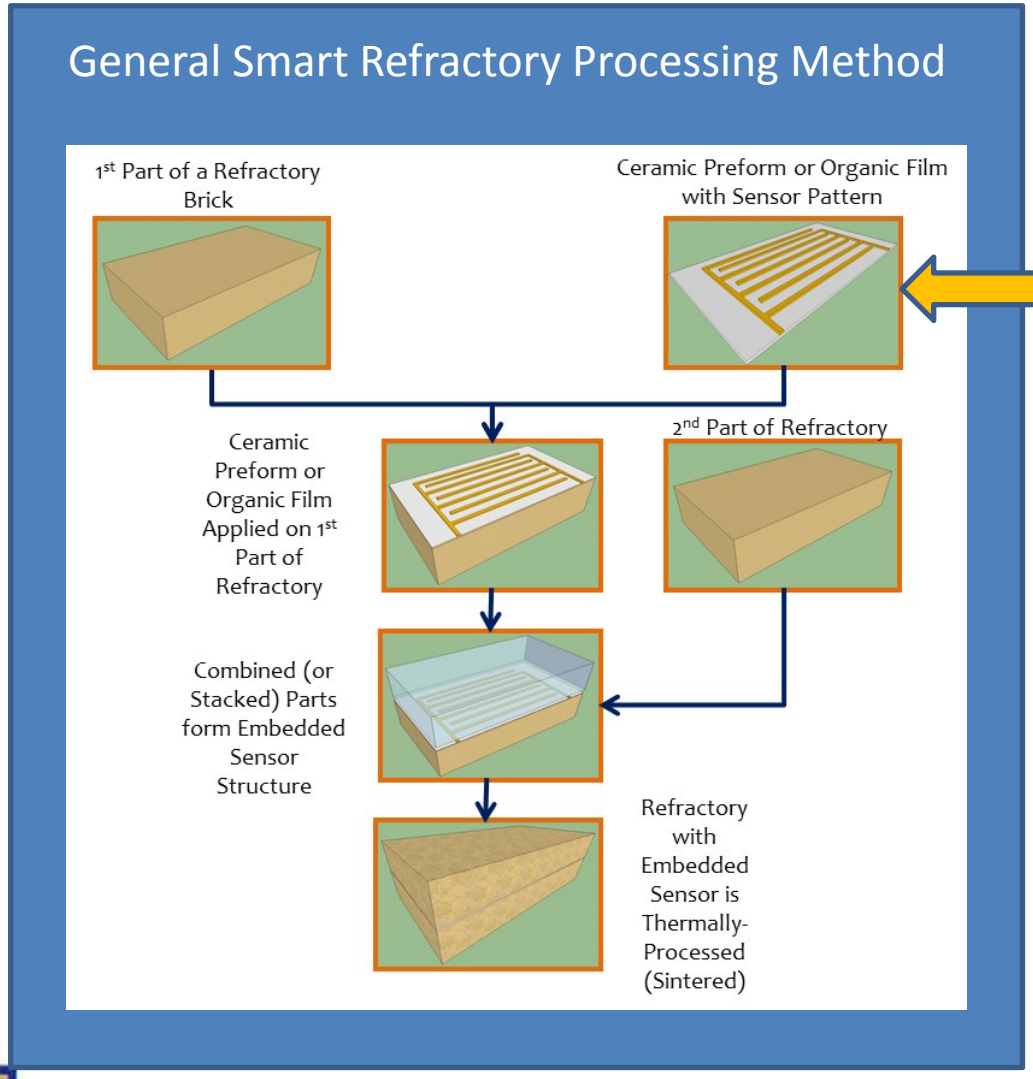

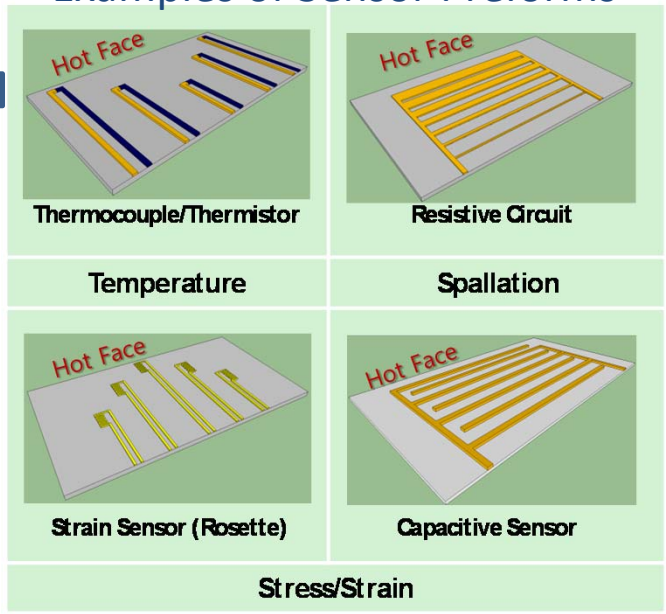

High-Temperature Thermocouple Performance:

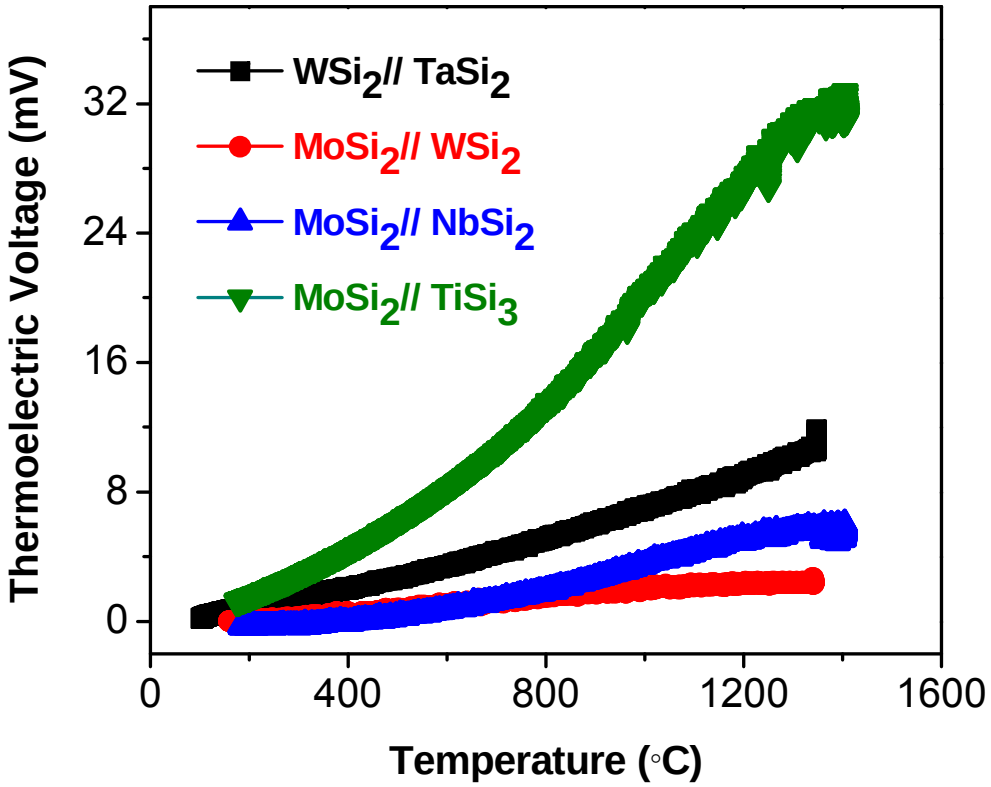

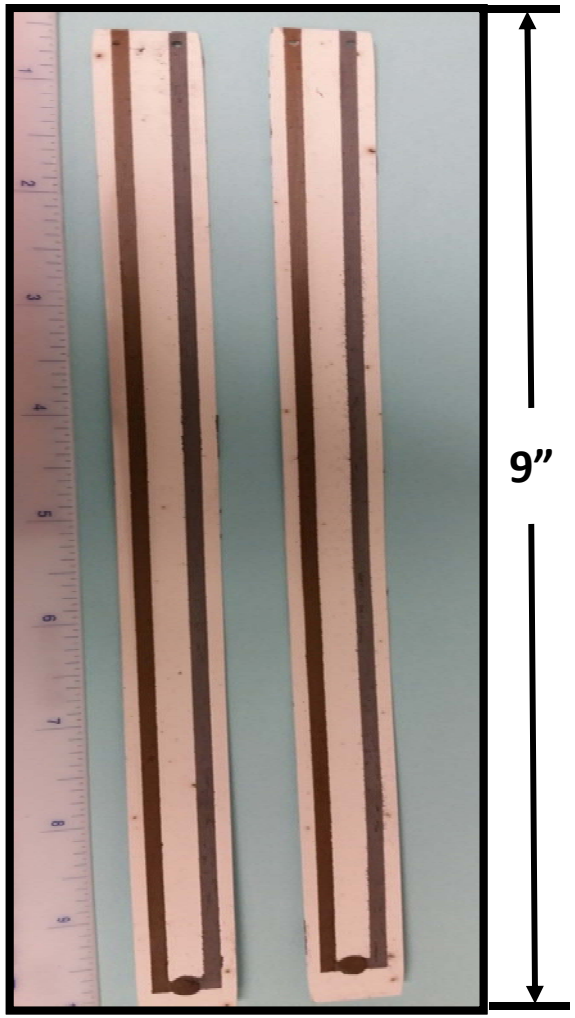

Various thermocouple compositions studied at 1500 °C

90 vol% silicide and 10 vol% oxide

The thermocouple with composition $MoSi_2$ //$TiSi_2$ exhibited 34 mV at 1400 °C

Long Thermocouple Preforms:

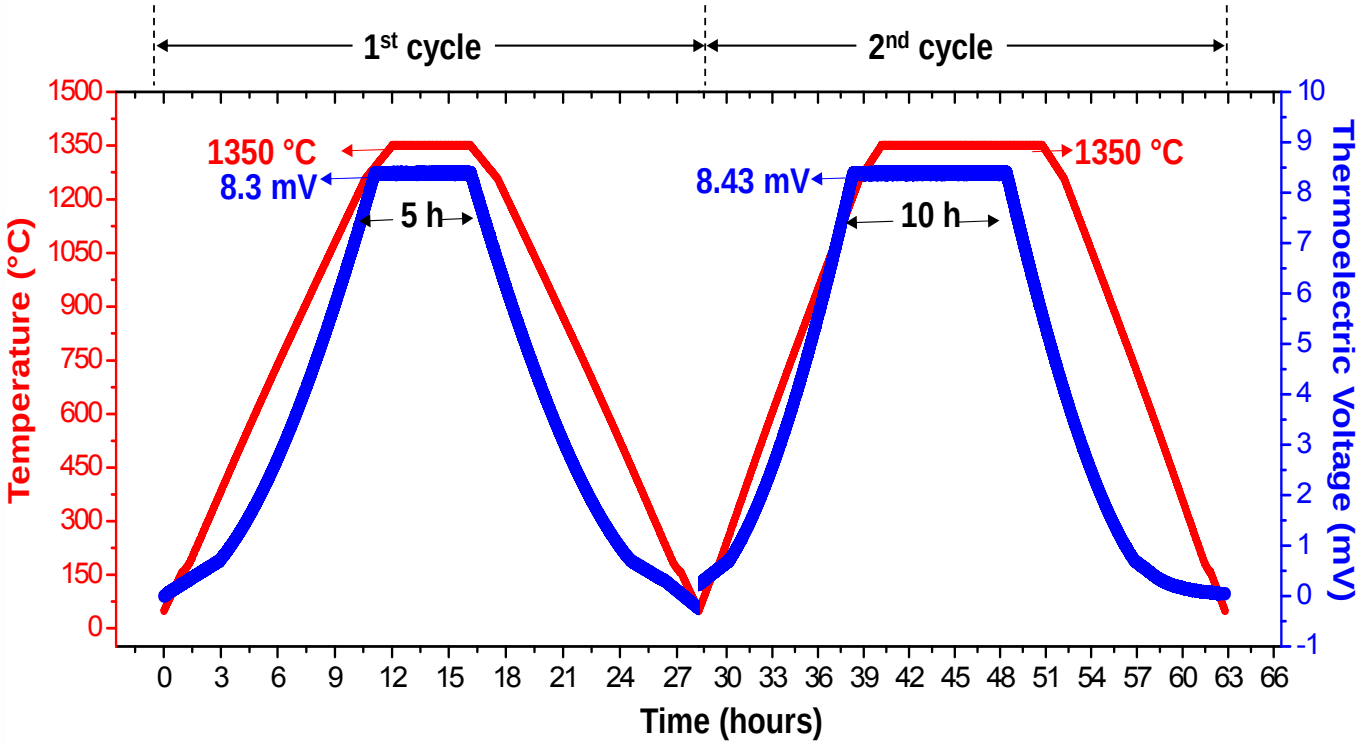

Long Thermocouple: [75-25] Vol% $MoSi_2$-Al_2O_3//[75-25] Vol% WSi_2-Al_2O_3 laminated between alumina substrates and sintered at 1500 °C, 2h in argon and tested isothermally at 1350 °C for 2 cycles in argon atmosphere

Temp. °C	Experiment	Hold Time, h	EMF, mV
1350	Cycle # 1	5	8.3
1350	Cycle # 2	10	8.43

TC: [75-25] Vol% $MoSi_2$-Al_2O_3// WSi_2-Al_2O_3

Smart Refractory Microstructure:

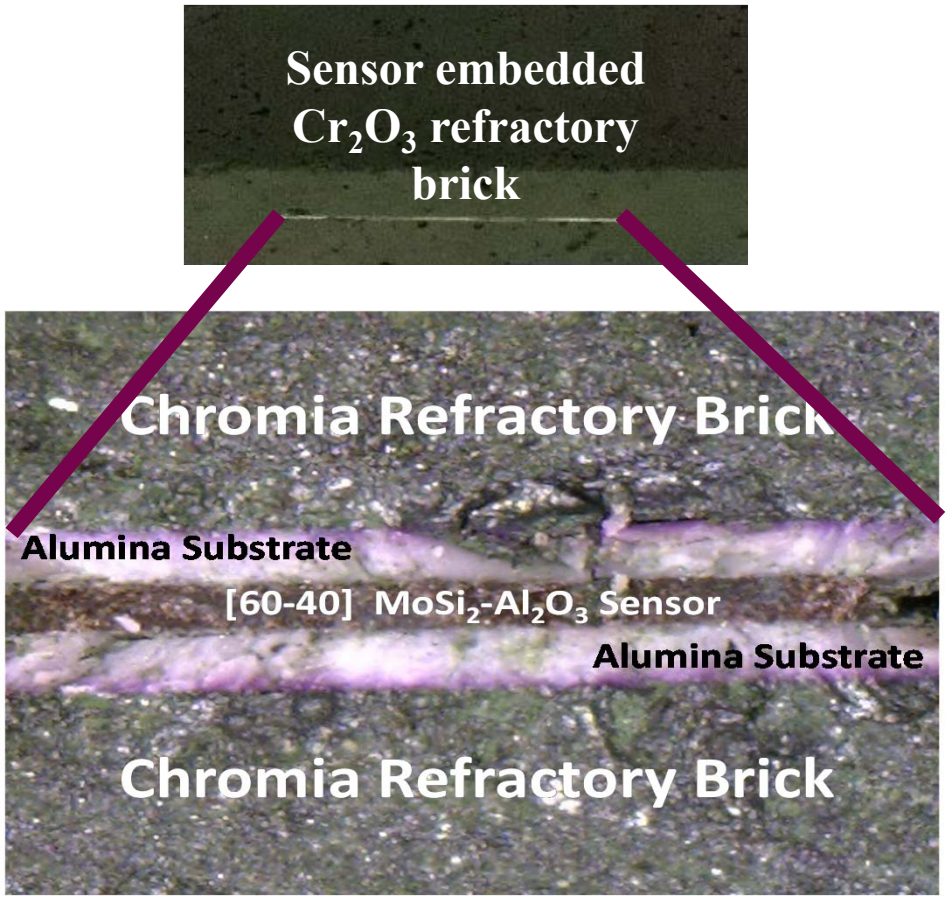

- Monoliths of sensors were fabricated via tape casting, laminated and sintered at 1500 °C. These laminates were embedded in the Cr_2O_3 brick while slip casting and co-sintered at 1500º C in Argon atmosphere.

Embedded Thermocouple: Smart Chromia Brick

- Sensor preform embedded HWI high-chromia formulation.
- Sensor embedded below opening to insert slag composition for corrosion testing.

Long TC embedded Chromia Refractory Brick

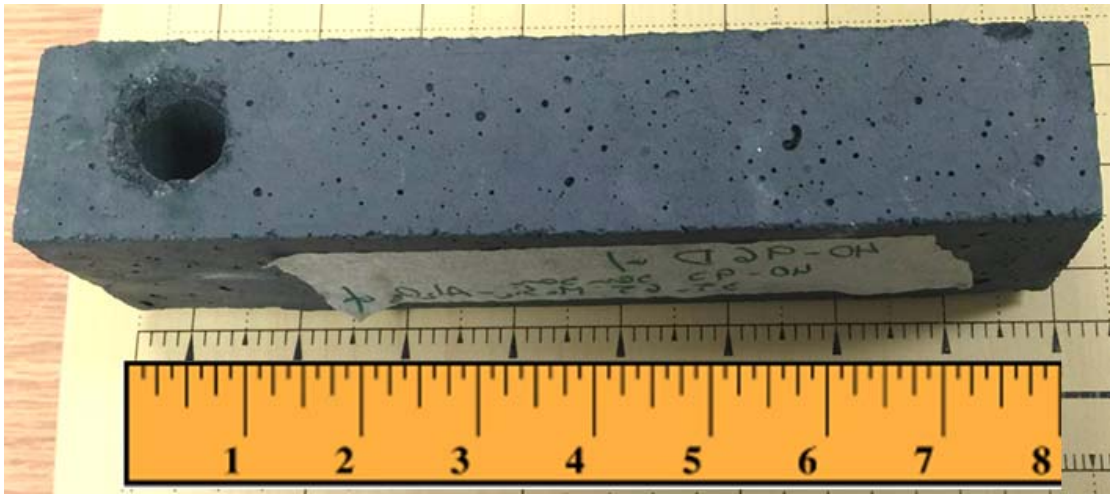

Thin Embedded TC Sensor

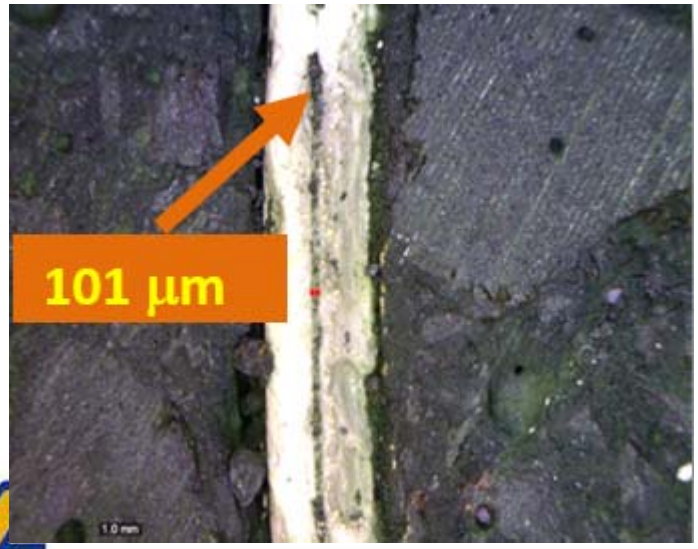

Interfaced Smart Brick

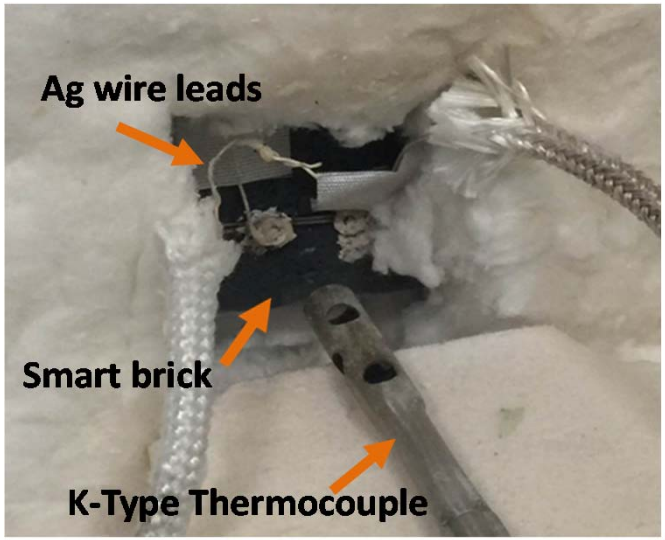

Embedded Thermistor: Smart Chromia Brick

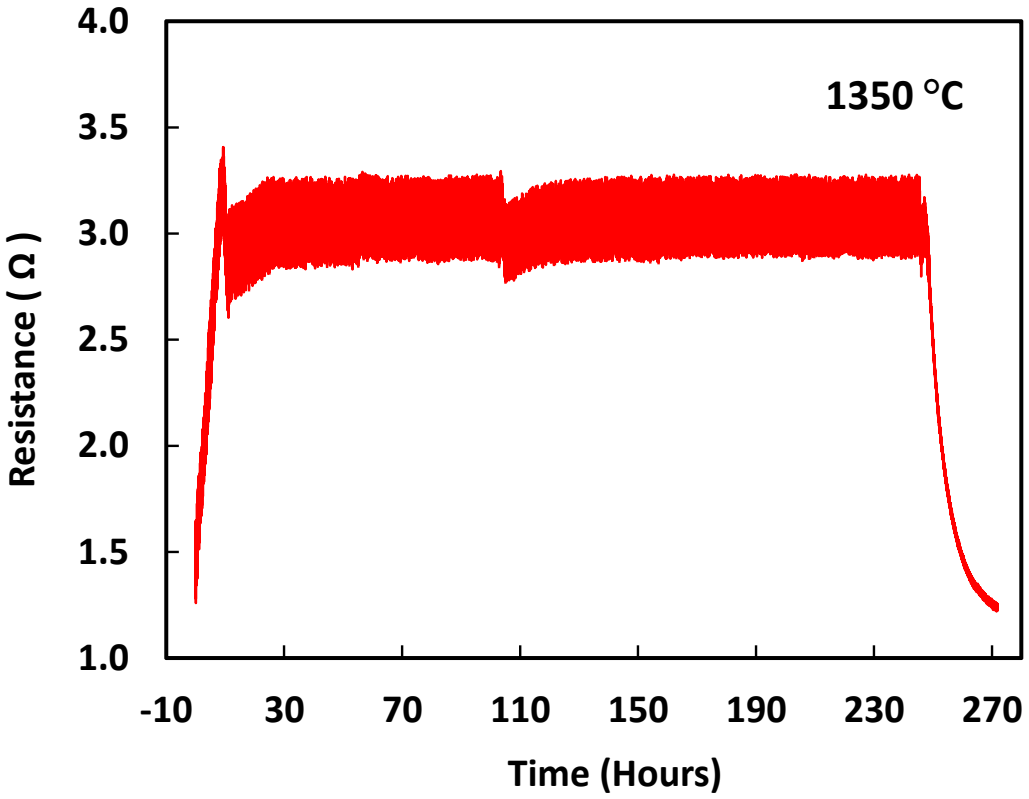

Performance of thermistor [60-40] vol% $MoSi_2$-Al_2O_3

Thermistor embedded smart brick in the testing furnace

- The temperature sensor (thermistor) with composition (60-40) vol% $MoSi_2$-Al_2O_3 embedded within the Cr_2O_3 refractory exhibited stable behavior for more than **250 hours at 1350 °C** in argon atmosphere.

Static and Dynamic Corrosion Tests: (Currently On-going)

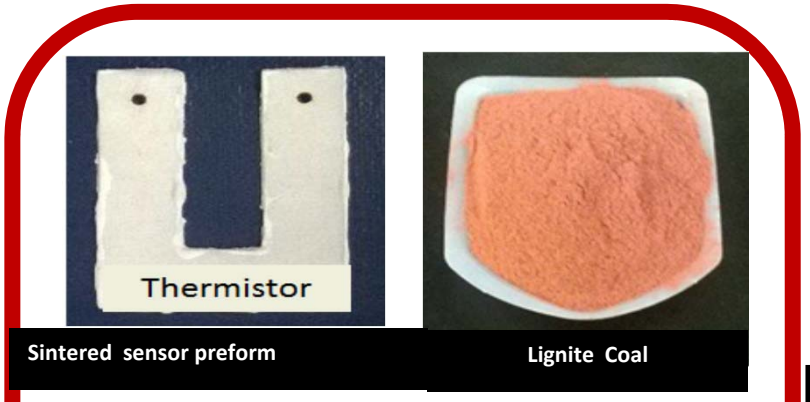

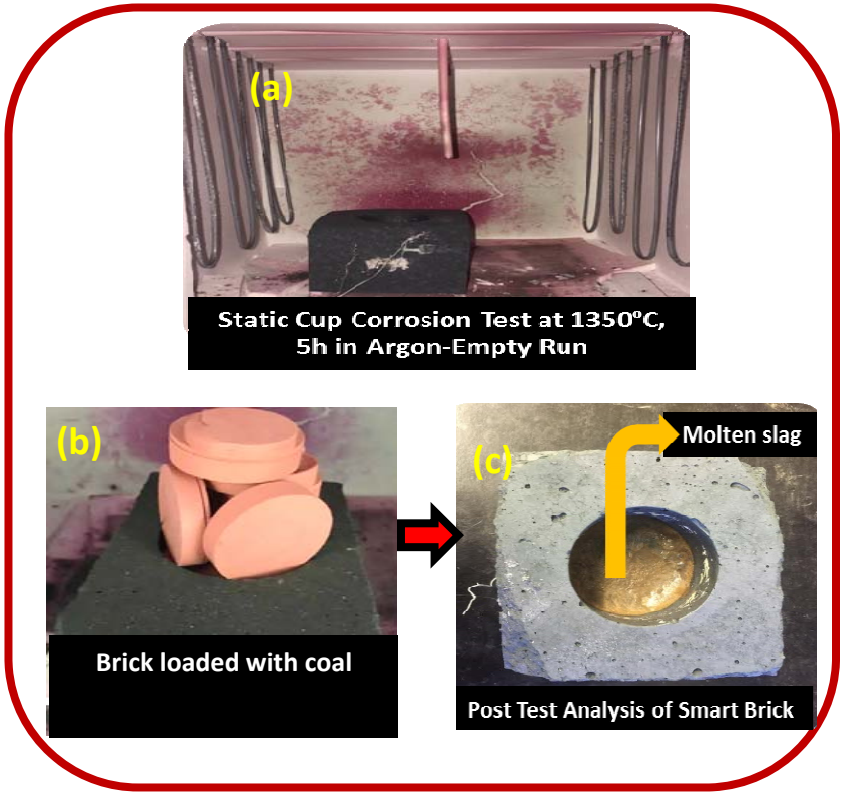

- Various steps involved in the testing of smart refractory brick embedded with [90-10] $MoSi_2$-Al_2O_3 thermistor and tested at 1350 ºC , 2h in Argon

Lignite Coal Slag→ 44.3SiO_2-5.26Fe_2O_3-17.5CaO-6.64MgO

Current Issue: Brick Interconnection

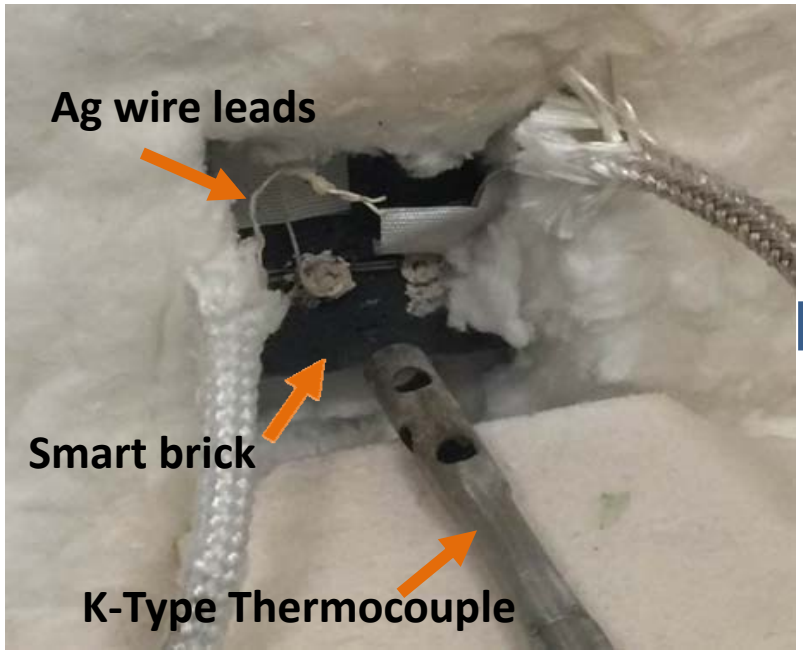

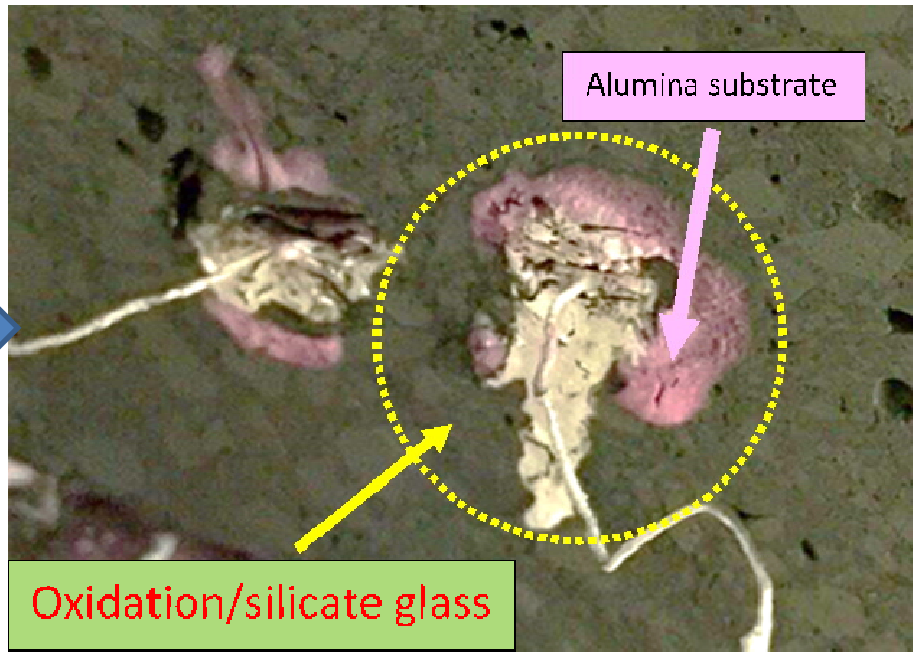

- Loss of electrical connection to bricks during testing.
- Metal lead delamination due to wetting limitations.
- Phase oxide formation in locations that are not embedded causing drift in response.

Efforts are focusing on better understanding the issue and developing the proper ceramic and/or metal connections.

Task 3 and 4 Conclusions and Future Work:

- All-ceramic thermocouple and thermistor preforms were fabricated and successfully tested.
- Smart high-chromia bricks were fabricated in collaboration with HWI (both thermistors and thermocouples), and currently going under test.

Future Work:

- Optimize method to interconnect to embedded sensors (in order to stabilize sensor signal and sensor long-term response).
- Investigate the corrosion/erosion kinetics of sensor embedded refractory bricks in static and dynamic mode with slag.
- Scale-up all sensor preforms and smart refractory brick for **FULL-TECHNOLOGY DEMO IN TASK 7**.

Task 5:
Data Ex-Filtration Using a Wireless Sensor Network.
*(*Graham/Kulathumani*)*

HWI

Task 5 Objectives:

- To develop methods to interface the electrical sensing outputs from the smart refractory with an embedded processor
- To design a wireless sensor network to efficiently collect the data at a processing unit for further data analysis

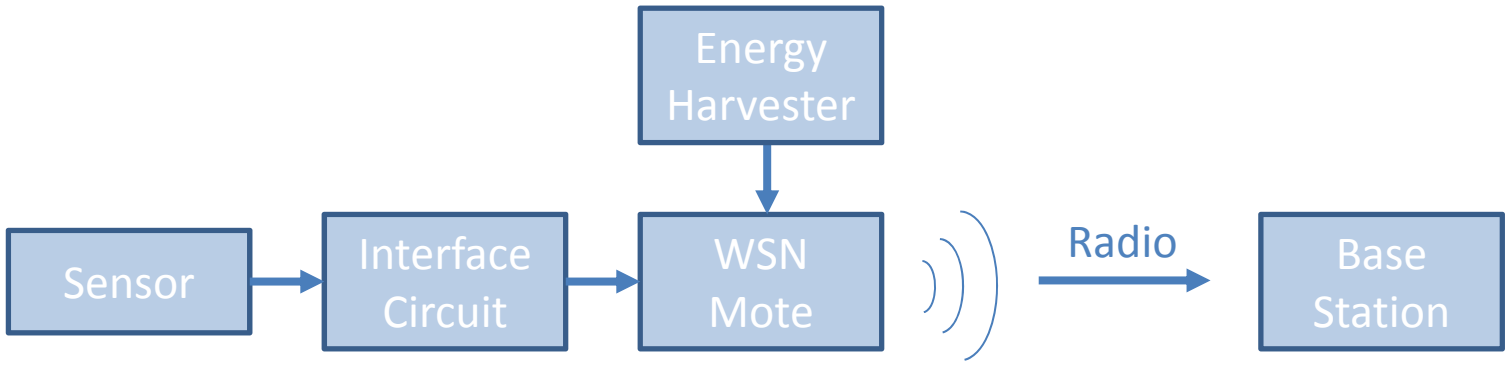

Electronics interfacing – Approach:

Aim: To reliably collect data from the sensors embedded within the smart bricks and interface them to wireless sensor nodes for communication

Approach:

(i) Iterative approach to sensor interface circuitry in parallel with the sensor development

a) Initial sensor interface circuitry using off-the-shelf circuitry

b) Move to integrated circuits for lower-power and more compact solutions

(ii) Investigate energy harvesting using thermoelectric devices to help power the sensor motes and interface circuitry

HWI

Custom Integrated Circuit:

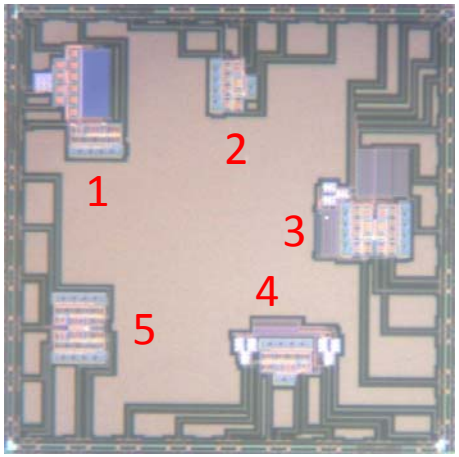

1. Cold-Junction Compensator
2. Thermocouple Amplifier
3. Capacitive Sensor
4. Thermocouple Amplifier V2
5. Wheat-Stone Bridge

Resistance-Based Sensor

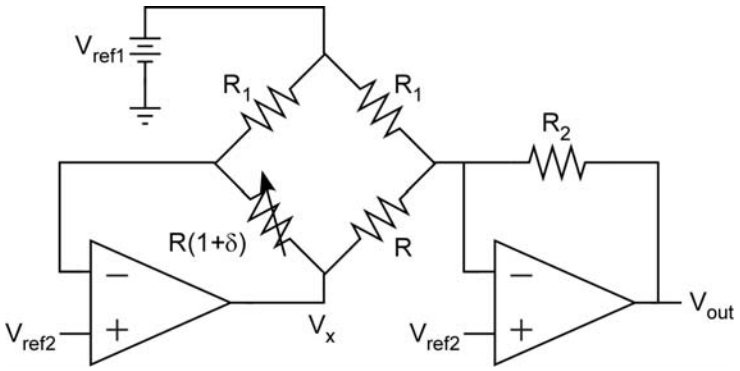

$$V_{out} = V_{ref2} + \frac{R_2}{R_1}\delta\left(V_{ref1} - V_{ref2}\right)$$

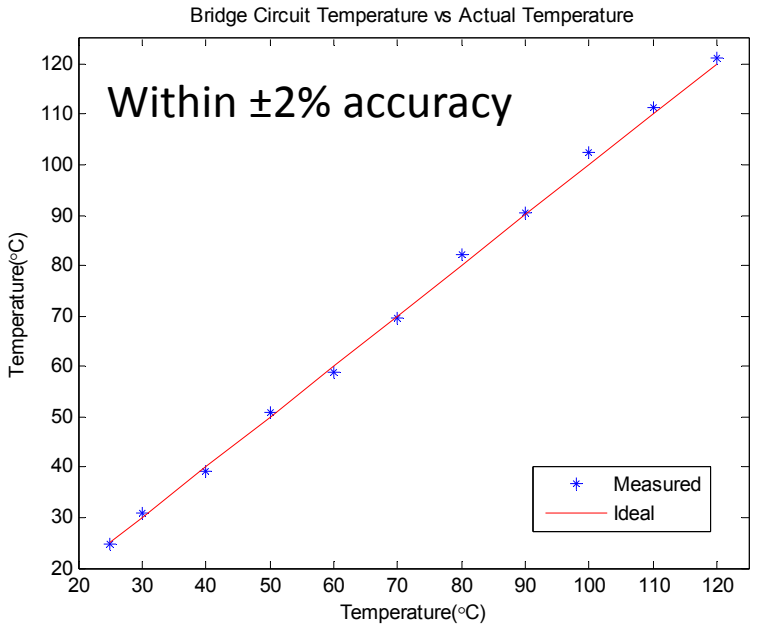

Circuits for Thermocouple-Based Sensors:

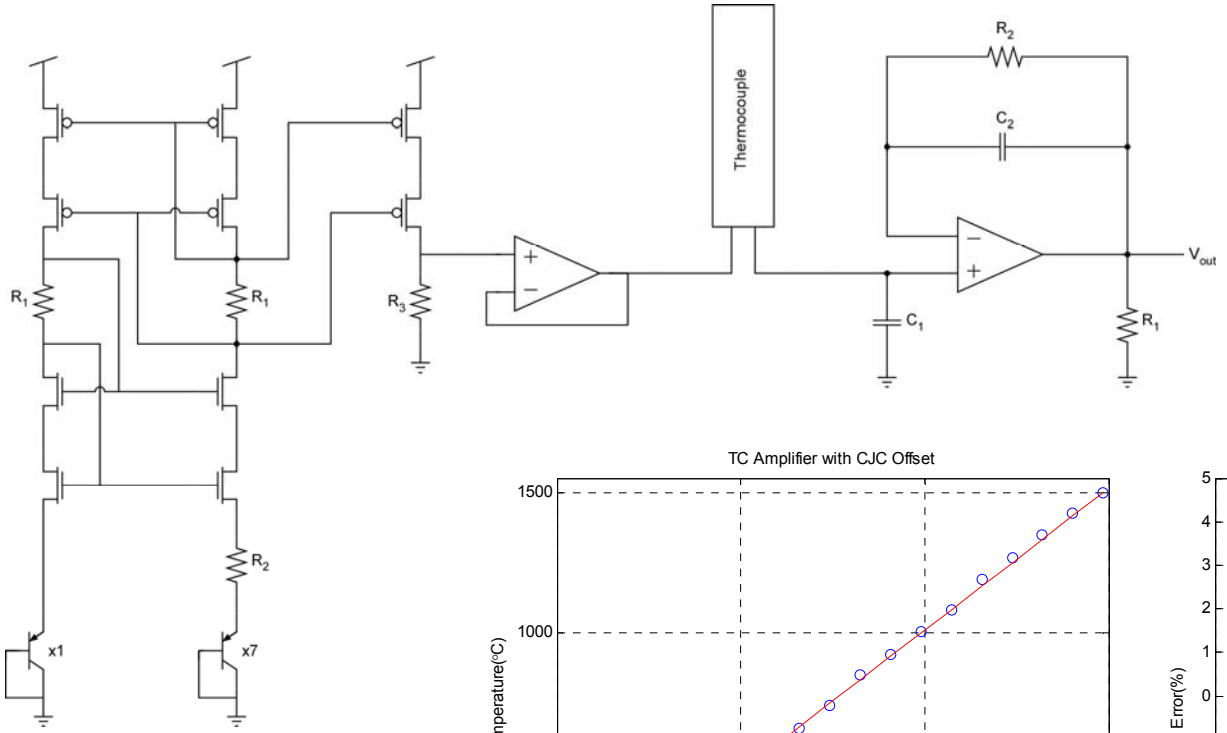

- Compensates for measurement error at thermocouple cold junction
- Adds offset to thermocouple input to allow for the correct temperature measurement
- Greatly improves accuracy over a large range of temperature values

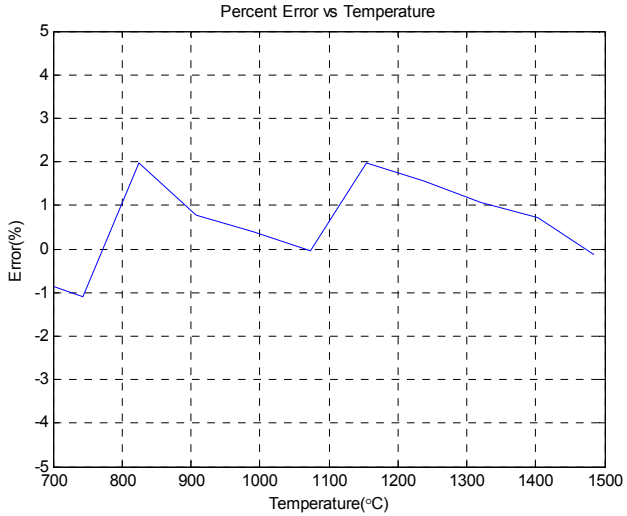

Circuits for Energy Harvesting:

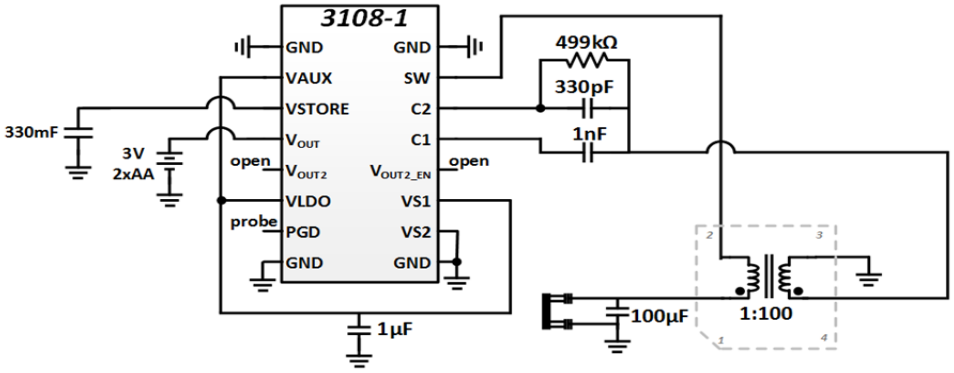

- Leverages COTS-based DC/DC converter circuit (LTC3108)
- Start-up Sequence shows the output of Thermoelectric Generator, LDO Regulator, Storage Buffer, and V_{OUT}.
- The Mote Experiment was done using a TelosB. The results shown are 10 minutes into the test. Once a minute, the TelosB turned on and was powered by the energy harvesting system for a 5 second radio transmission.

V_{OUT} – System Output
Storage Buffer – Energy Storage Output
LDO Regulator – Internal Regulator Output
TEG – Thermoelectric Generator Output

Start-up Sequence

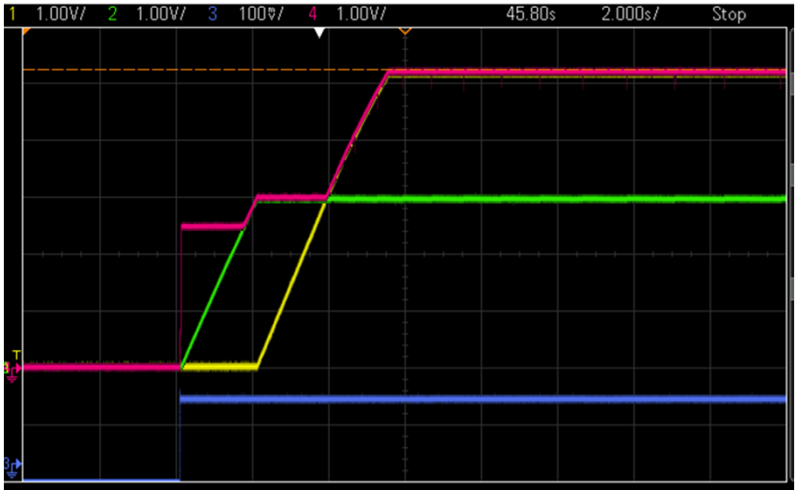

Mote Experiment: Testing Results

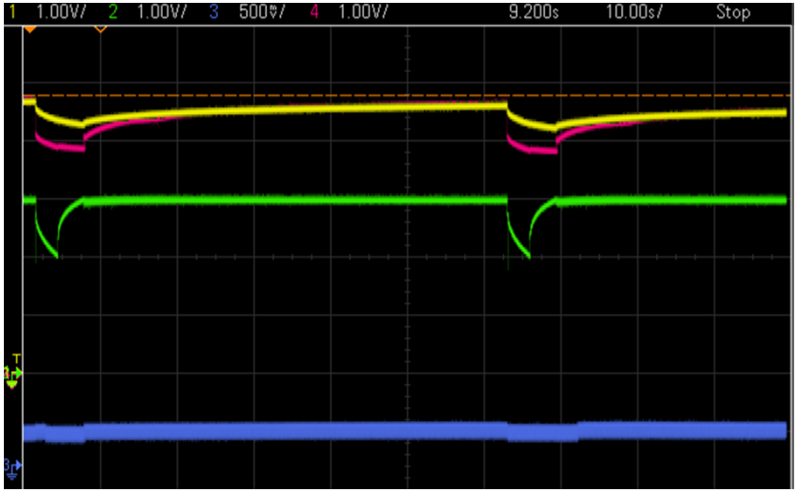

Wireless sensor network overview:

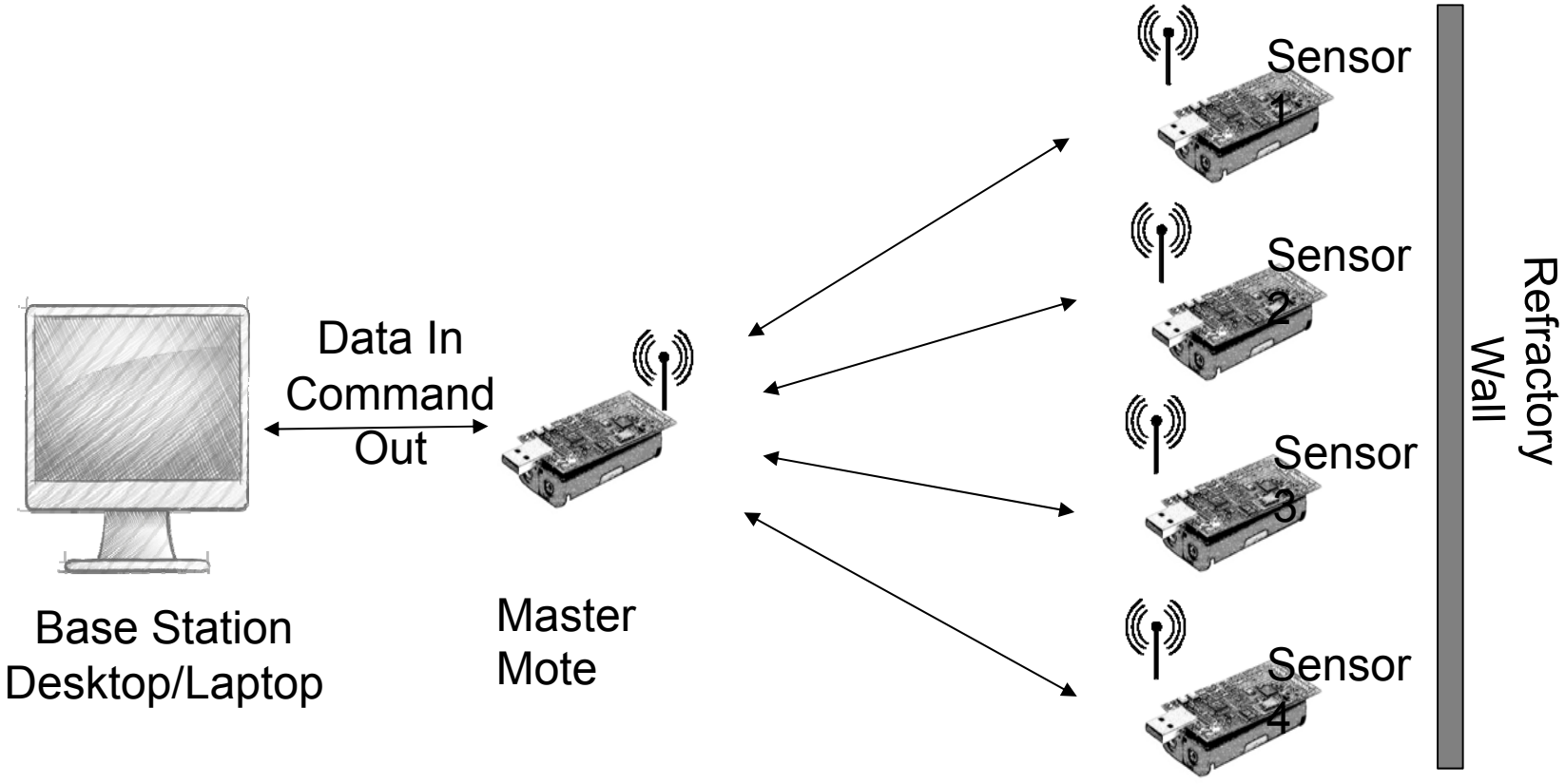

- Collect refractory sensor data over wireless medium
- (data ex-filtration)
- Enable remote configuration of parameters
  - (over-the-air programming)

Assembled complete signal chain:

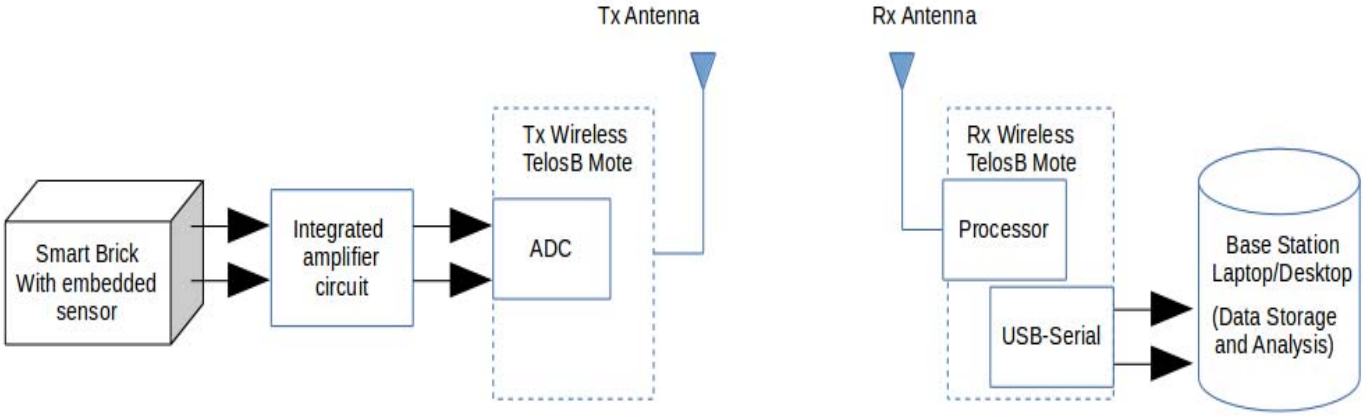

- Smart bricks with embedded sensors were interfaced with a wireless mote yielding a complete signal chain comprising
  - the smart brick,
  - resistance measurement / amplifier circuit,
  - and wireless data transmission.

Verified wireless signal chain performance:

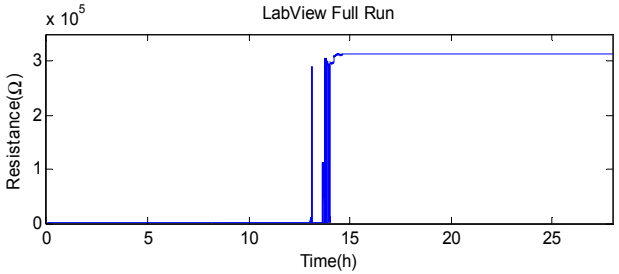

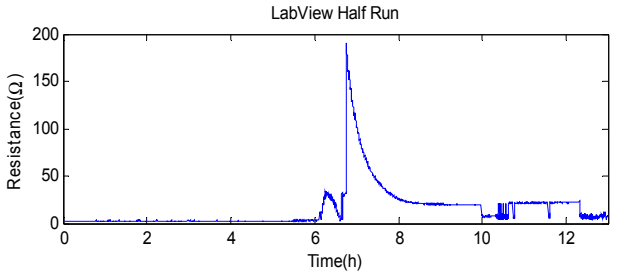

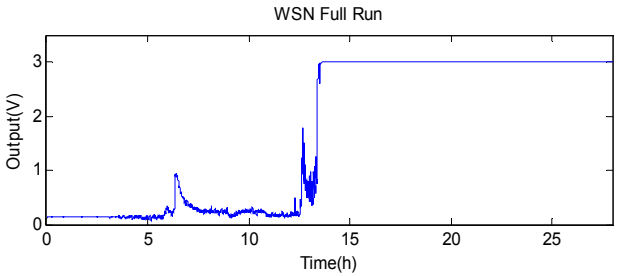

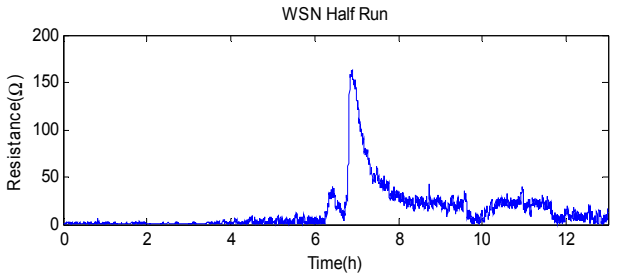

- Wireless Sensor Network (WSN) data collected from smart bricks by measuring voltage from ICs [bottom figure]
- Resistance measured directly on Labview by connecting an ADC probe [top figure]
- Figures show similar trend, thus verifying correctness of the wireless network based data collection

Results on increasing scale of network:

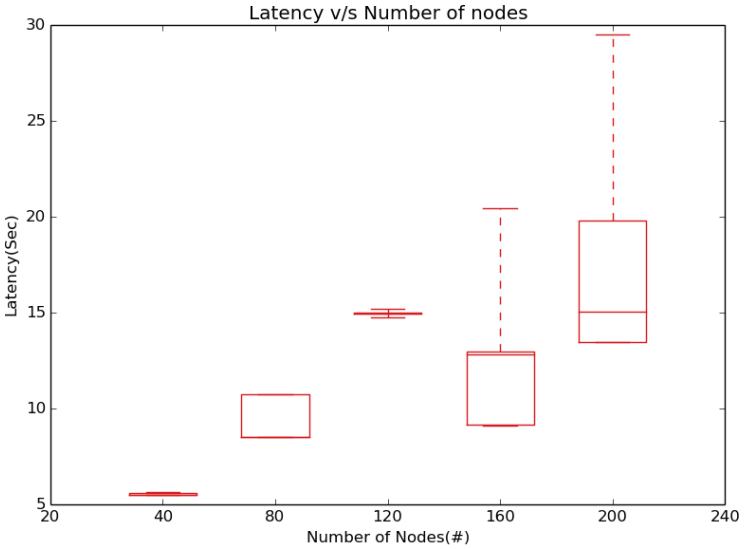

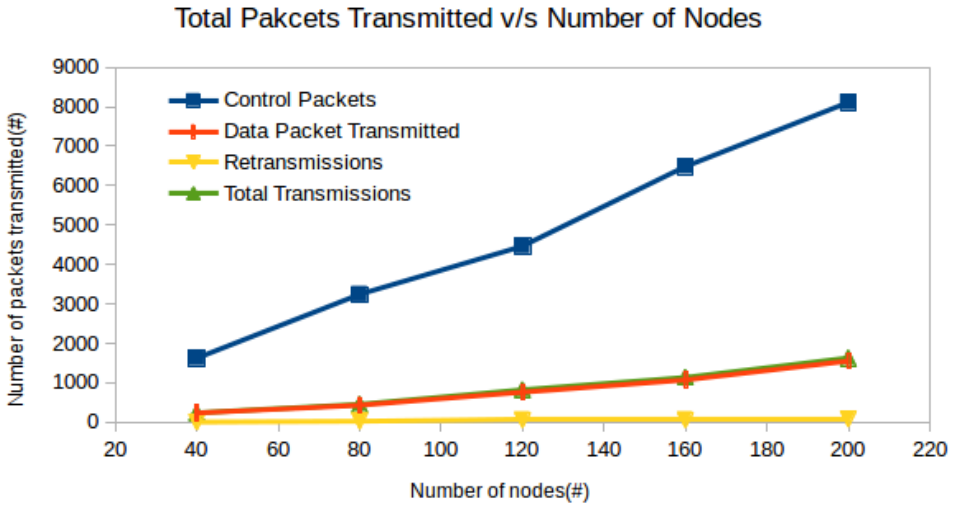

- Tested ability of sensor network protocol to handle larger network sizes
  - Evaluated sizes from 40-200 using a ns-3, a network simulator
  - Customized collection tree protocol to periodic data collection scenario
  - 100% data reliability
  - Latency and message size grow linearly with network size

Task 5 Conclusions and Future Work:

- The end to end signal chain for data collection system has been implemented and tested using actual smart brick prototypes
  - Sensors are interfaced with microcontroller + radio (motes)
  - Data collection protocol has been implemented
  - Visualization and sensor control interfaces have been implemented
- Scalability of network protocol was evaluated
- Refinements to interface circuits to suit updated sensors
- Model based data reduction techniques are being explored
  - This can help reduce data rate without compromising with information required for analyzing system characteristics.

HWI

Task 6.0: Model-Based Estimation of Temperature Profile and Extent of Refractory Degradation.

*(*Bhattacharyya, Huang*)*

Task 6 Objectives:

- To develop algorithms for model-based estimation of temperature profile in the refractory, slag penetration depth, spallation thickness, and resultant health by using the data from the wireless sensor network

Motivation:

- Typical correlation based approaches are inadequate
- Stiff temperature gradient along the refractory resulting in a large temperature change along the sensor length
- Change in thermal and electrical properties over time due to slag penetration

Property Models:

In order to build the model of smart refractory , several temperature-dependent property models for refractory or sensor material are needed:

- Specific heat
- Emissivity
- Thermal conductivity
- Electrical conductivity
- Thermal expansion
- Dielectric constant
- Young's modulus
- Poisson's ratio

The electrical resistivity model for refractory*

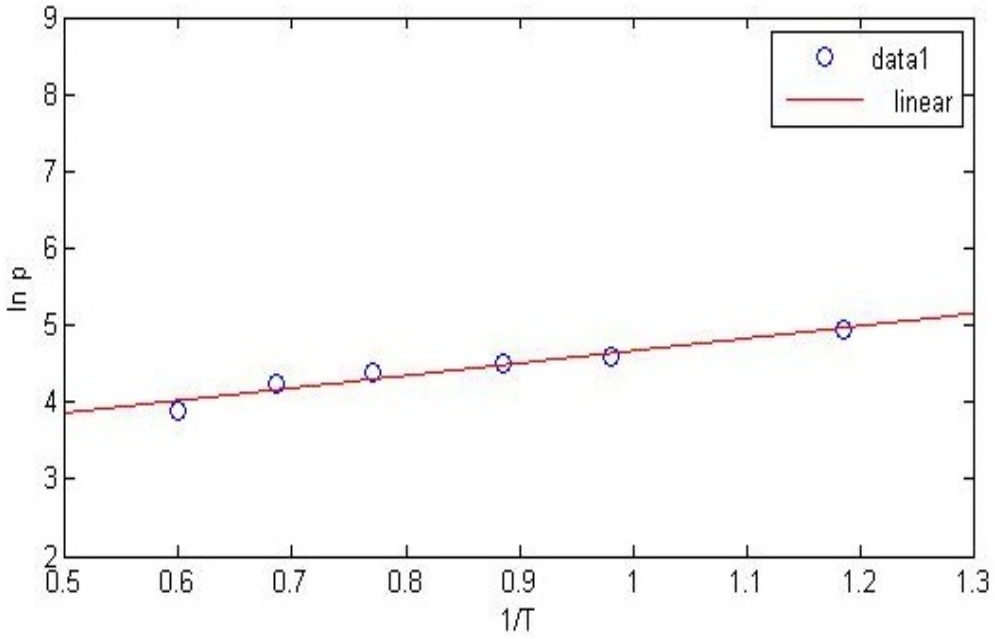

*Hensler J R, Henry E C. Electrical Resistance of Some Refractory Oxides and Their Mixtures in the Temperature Range 600° to 1500° C[J]. *Journal of the American Ceramic Society*, 1953, 36(3): 76-83

Property Models for Composite:

The properties of refractory will change as the slag penetrates into the wall. These models can be used to predict the effective properties of a special kind of composite(slag and the refractory).

- Specific heat
- Thermal conductivity
- Dielectric constant

Thermal Model of a Gasifier Wall:

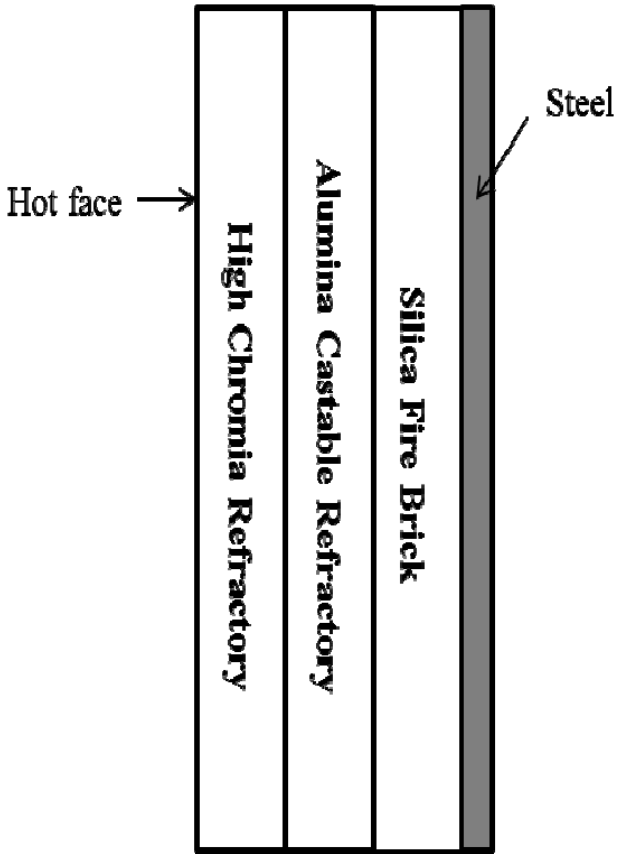

2-D heat conduct equation was used:

$$\frac{\partial T}{\partial t} = \frac{K}{\rho C_p}\left(\frac{1}{r}\frac{\partial}{\partial r}\left(r\frac{\partial T}{\partial r}\right) + \frac{\partial^2 T}{\partial z^2}\right)$$

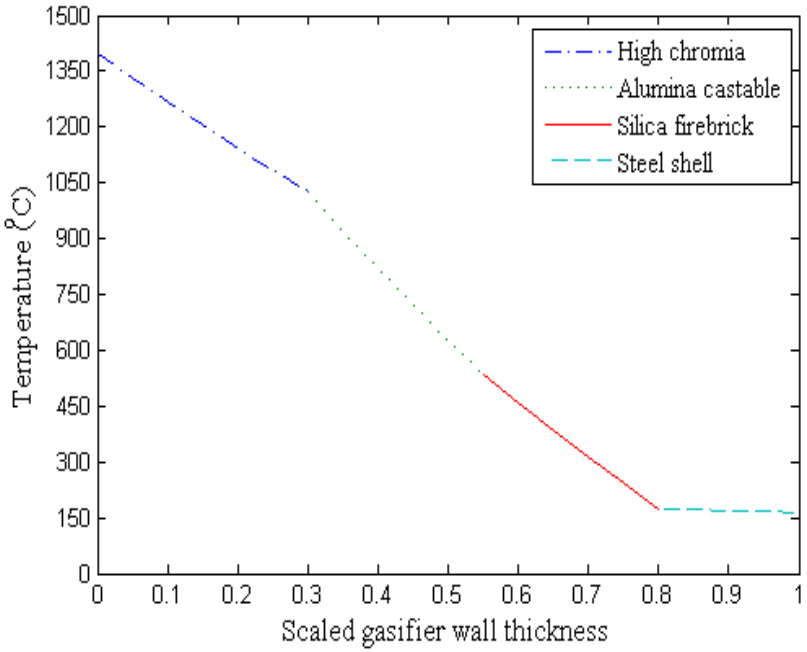

Slag Penetration Model:

Velocity of capillary flow through the horizontal pores (Washburn, 1921)

$$\varphi = \frac{\Delta P r^2}{8\eta l}$$

Corrected by porosity and tortuosity of the refractory pore system. (Williford et al., 2008)

$$l = \sqrt{\frac{\Delta P r^2 \phi}{8\eta\sigma}}$$

- Velocity of slag penetration decreases quickly
- Temperature gradient

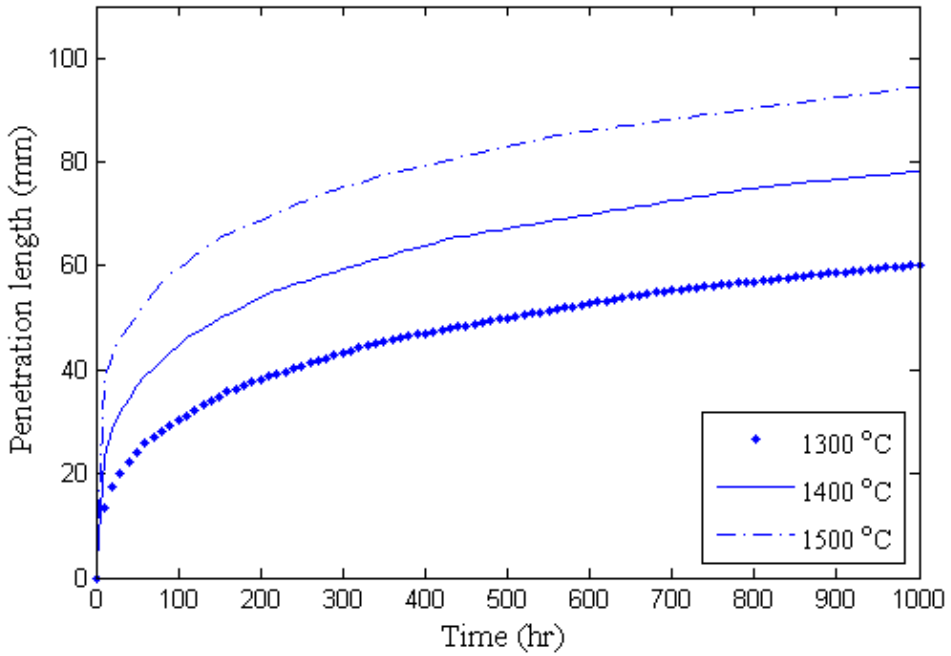

Williford, R. E.; Johnson, K. I.; Sundaram, S. K.; Pilli, S. Effective diffusivity and spalling models for slagging coal gasifiers. J. Am. Ceram. Soc. 2008b, 91, 4016-4022.

Sensor Models:

Five different types of sensors:

- Interdigital capacitor (IDC)
- Strain gauge
- Resistive circuit
- Thermistor
- thermocouple

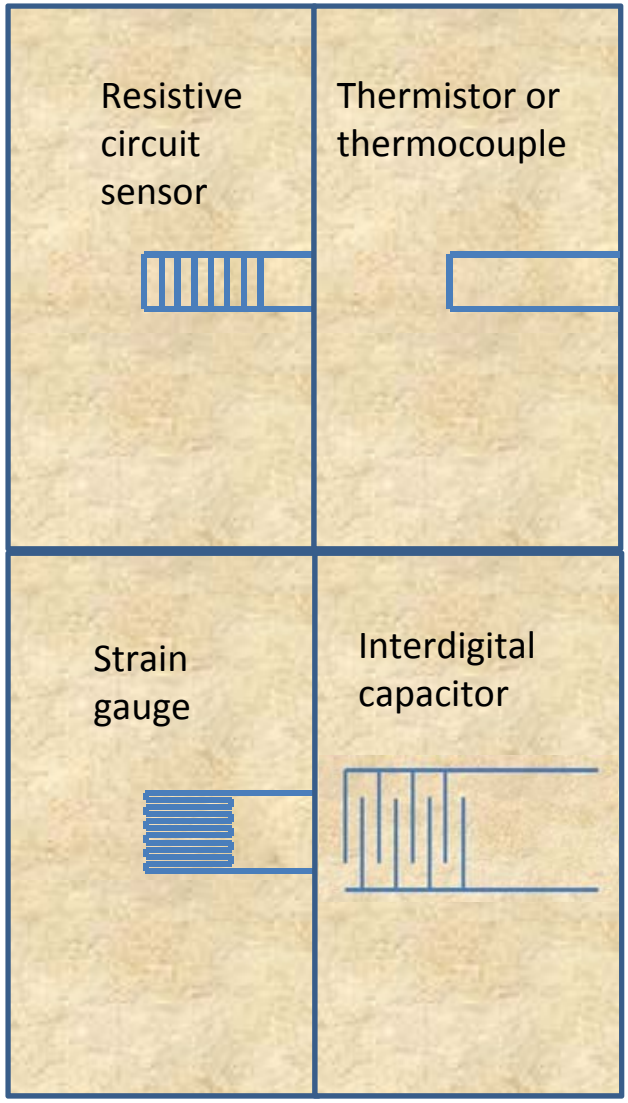

Interdigital Capacitor (IDC) Sensor Model:

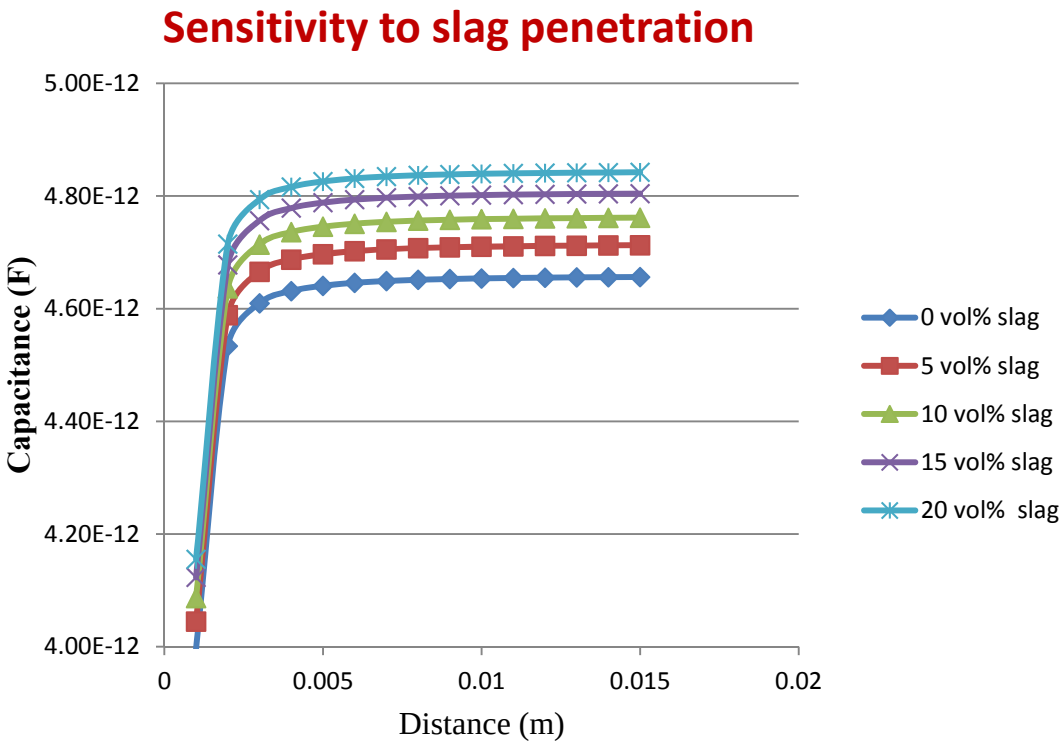

- Composite property model
- Slag can only fill the pores

* Igreja R, Dias C J. Analytical evaluation of the interdigital electrodes capacitance for a multi-layered structure[J]. Sensors and Actuators A: Physical, 2004, 112(2): 291-301.

Estimation:

Methods:

- Traditional Kalman Filter (TKF)
  - Linear process model
  - Computationally cheap
  - Less accuracy for highly nonlinear process
- Extended Kalman Filter (EKF)
  - Nonlinear process linearized at every time step
  - Computationally costlier than TKF
  - Higher accuracy than TKF for nonlinear process
- Unscented Kalman Filter (UKF)
  - Nonlinear process
  - Computationally expensive
  - Superior accuracy

HWI

Filter Algorithm:

- Differential Algebraic Equations System

Nonlinear differential algebraic equations (DAE) system:

$$\dot{x} = \bar{F}(x, z) + \gamma$$
$$\bar{0} = \bar{G}(x, z)$$
$$Y = H \begin{bmatrix} x \\ Z \end{bmatrix} + \omega$$

- Developed approach for handling the DAE System:

Linearized process model:

$$\dot{x} = A\,\Delta x + B\Delta z + E\,\Delta u$$
$$0 = C\,\Delta x + D\,\Delta z + F\,\Delta u$$

Augmented form:

$$\begin{bmatrix} \dot{x} \\ \dot{z} \end{bmatrix} = \begin{bmatrix} A & B \\ -D^{-1}CA & -D^{-1}CB \end{bmatrix} \begin{bmatrix} \Delta x \\ \Delta z \end{bmatrix} + \begin{bmatrix} E & 0 \\ -D^{-1}CE & -D^{-1}F \end{bmatrix} \begin{bmatrix} \Delta u \\ \dot{\Delta u} \end{bmatrix}$$

Estimation of Temperature Using EKF:

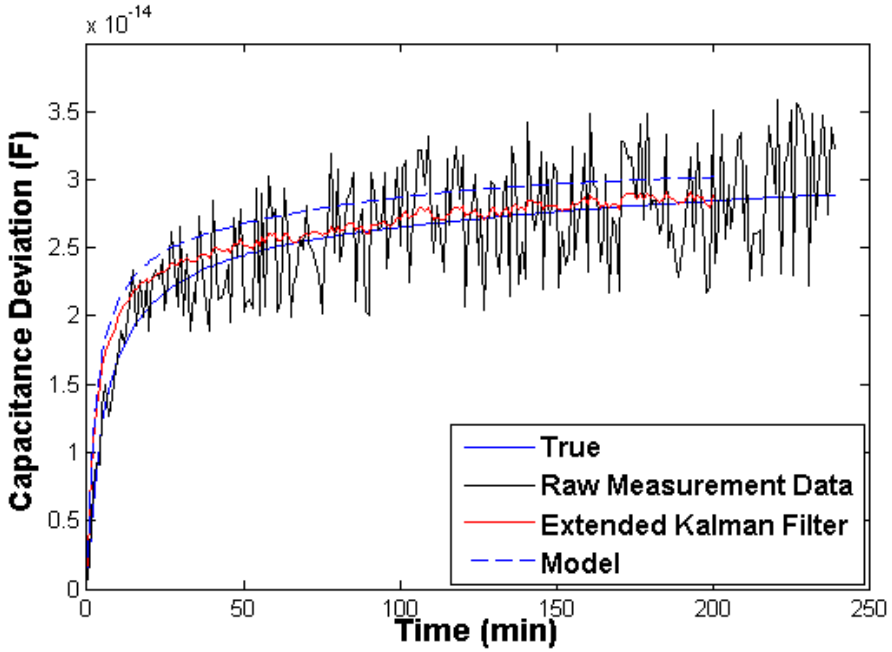

Estimation of capacitance

- Assume five IDC sensors are embedded diagonally in the refractory brick.

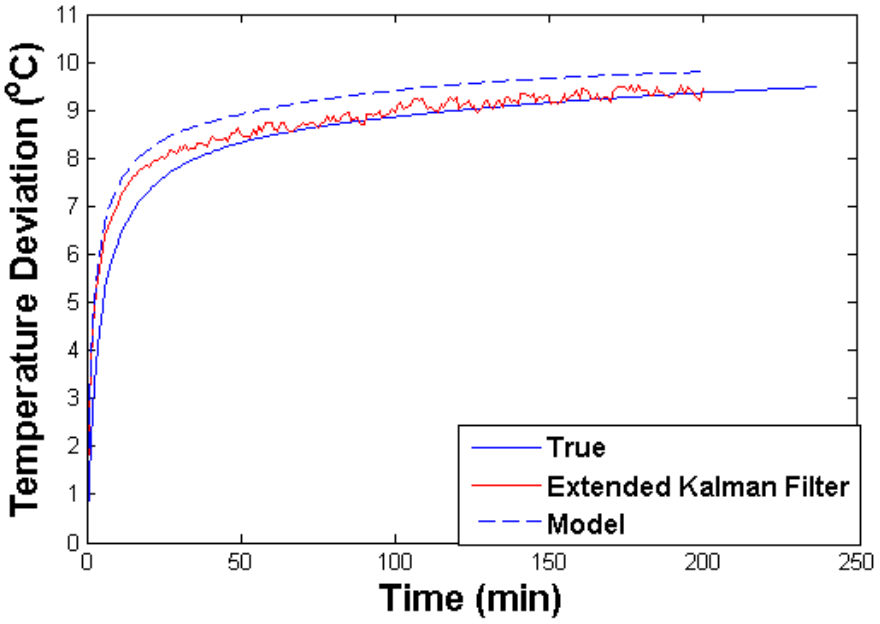

- Temperature Estimation for Different Extent of Slag Penetration are completed

Estimations of Temperature Using UKF:

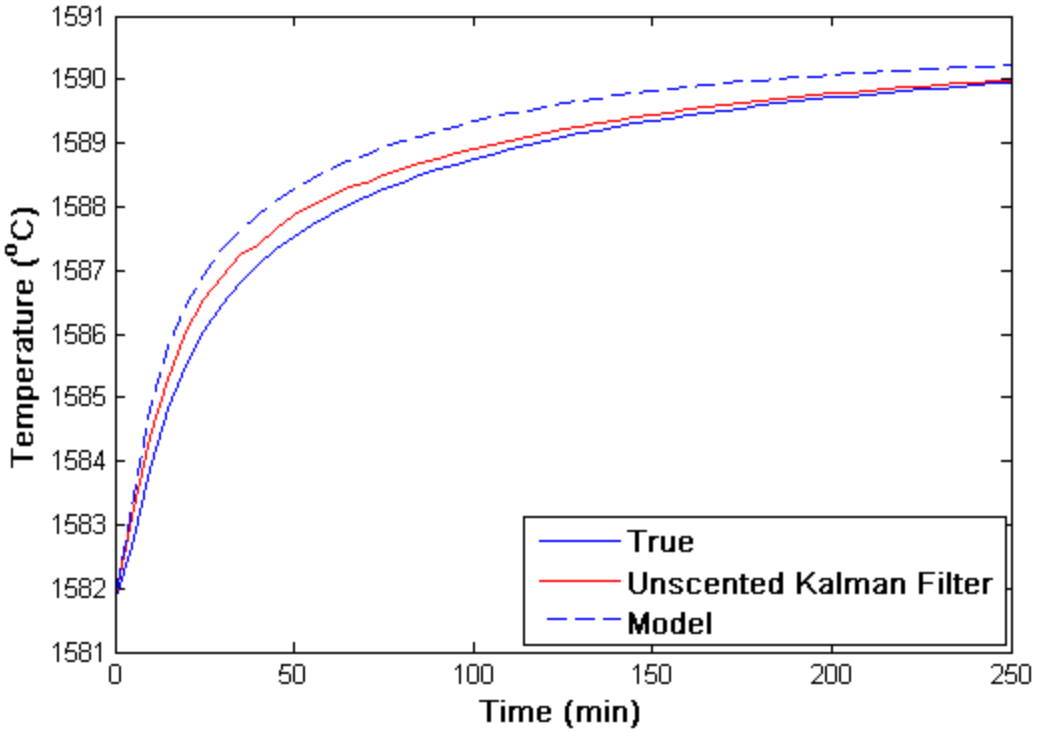

- Assuming five IDC sensors are embedded diagonally in the refractory brick

Estimations of Extent of Slag Penetration Using UKF:

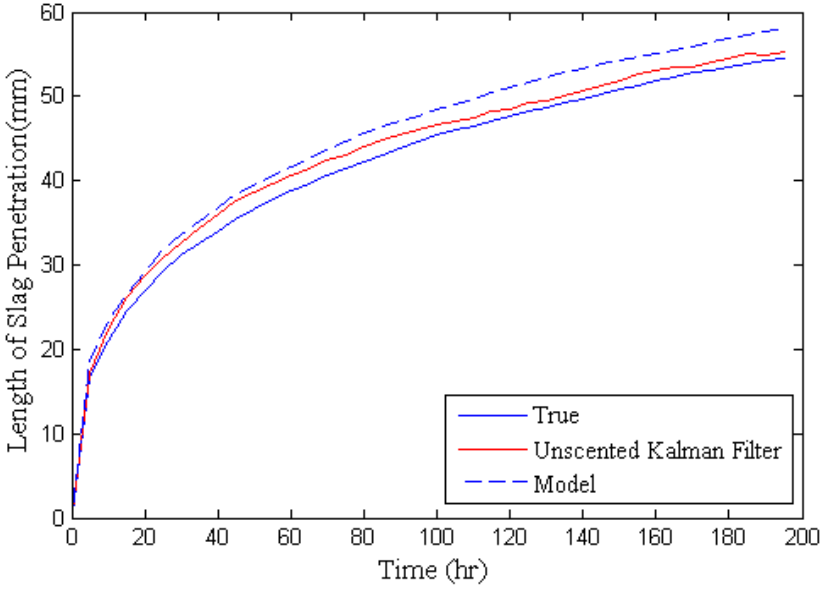

- Temperature is assumed to be under the normal operating conditions

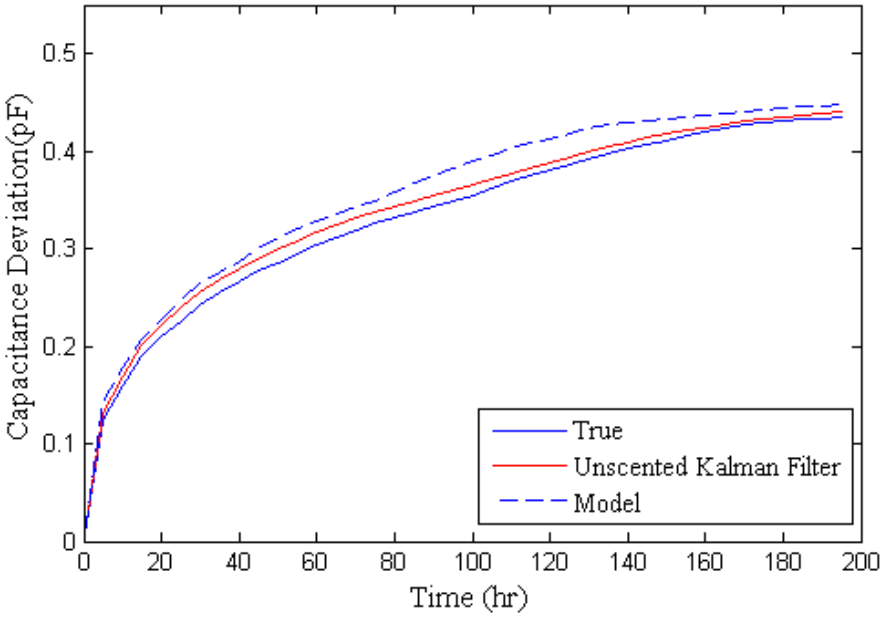

Task 6 Conclusions and Future Work:

- Nonlinear filtering algorithms have been developed to estimate temperature and the extent of slag penetration. The filters have been tested by using the data from the model of gasifier wall.

- Future work will focus on validation and testing of developed models and filtering algorithms using experimental data.

Products:

1. Edward M. Sabolsky, R. Chockalingam, K. Sabolsky, G. A. Yakaboylu, O. Ozmena, B. Armour, A. Teter, D. Bhattacharyya , David Graham , Vinod Kulathumani, Close Timothy and Marc Palmisiano, "Refractory Ceramic Sensors for Process and Health Monitoring of Slagging Gasifiers", 227th ECS Meeting- Chicago, Illinois, USA, May 28th, (2015).
2. Edward M. Sabolsky , R. Chockalingam, K. Sabolsky, G. A. Yakaboylu, O. Ozmen, B. Armour, A. Teter**,** D. Bhattacharyya, David Graham, Vinod Kulathumani, Close Timothy and Marc Palmisiano, "Conductive Ceramic Composites Used to Fabricate Embedded Sensors for Monitoring the Temperature and Health of Refractory Brick in Slagging Gasifiers," *XIVth International Conference European Ceramic Society*- Toledo, Espana 24th June, 2015
3. R. C. Pillai, E. Sabolsky, K. Sabolsky, G. Yakaboylu, B. Armour, J. Mayer, J. Bogan, M. Raughley and J. Sayre "Performance of high temperature ceramic-ceramic thermocouples embedded within chromia refractory bricks to monitor the health and stability of industrial gasifiers" Materials Science and technology MS&T2015, Oct 4-8, 2015, Greater Columbus Conventional Center, Columbus, Ohio, USA.
4. G. Yakaboylu, R. C. Pillai, B. Armour, K. Sabolsky, E. Sabolsky,"Development of Refractory Oxide/Metal Silicide Composites for High Temperature Harsh-Environment Sensor Applications",Materials Science and technology MS&T2015, Oct 4-8, 2015, Greater Columbus Conventional Center, Columbus, Ohio, USA.
5. G.A. Yakaboylu, R. C. Pillai, B. Armour, K. Sabolsky and E. M. Sabolsky, "Conductive Ceramic Composites for Fabricating High Temperature and Harsh Environment Sensors: Thermal Processing, Stability and Properties", *International Conference and Exposition on Advanced Ceramics and Composites*, January 24-29, 2016, Daytona Beach, Florida, USA.

Products:

6. R.C. Pillai, G.A. Yakaboylu, K. Sabolsky and E. M. Sabolsky,J. Bogan, J. Sayre, “Composite Ceramic Thermocouples for Harsh-Environment Temperature Measurements”, *International Conference and Exposition on Advanced Ceramics and Composites*, January 24-29, 2016, Daytona Beach, Florida, USA.
7. E. M. Sabolsky, R. C. Pillai, K. Sabolsky, G. A. Yakaboylu, B. Armour, A. Teter, M. Palmisiano and T. Close, “Refractory Ceramic Sensors for Process and Health Monitoring of Slagging Gasifiers”, *ECS Trans.*, Vol 66(37) pp 43-53 (2015).
8. B. Rumberg, D. Graham, S. Clites, B. Kelly, M. Navidi, A. Diello, V. Kulathumani, “RAMP: Accelerating Wireless Sensor Design with a Reconfigurable Analog/Mixed-Signal Platform”, Proceedings of the ACM/IEEE Conference on Information Processing in Sensor Networks (ISPN’15), pp. 47-58, Seattle, WA, April 13-16, 2015.

Appendix:

Thermocouple Microstructures:

Microstructure of ceramic-ceramic thermocouples sintered at 1500 °C in argon

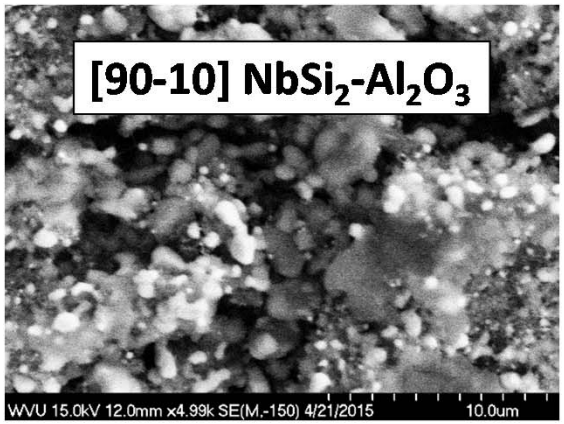

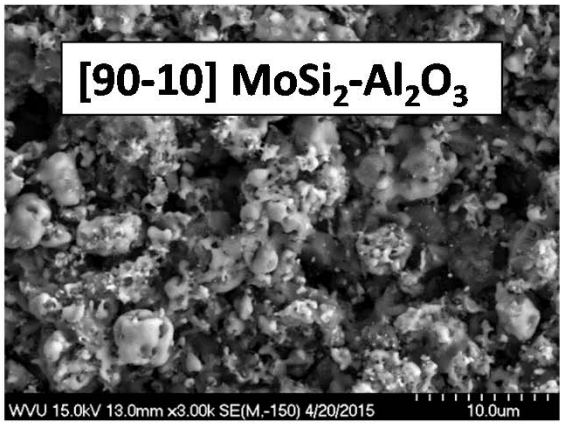

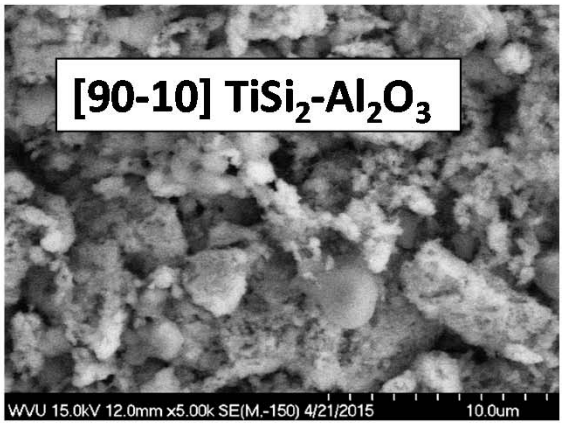

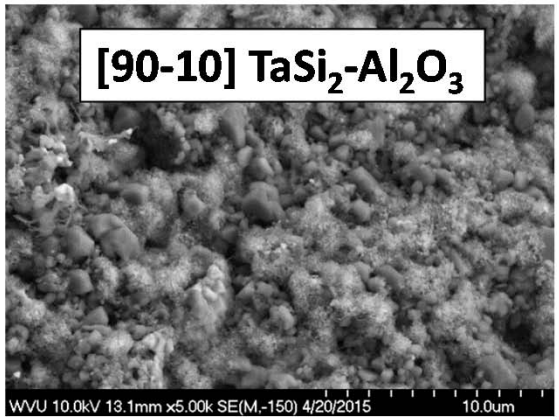

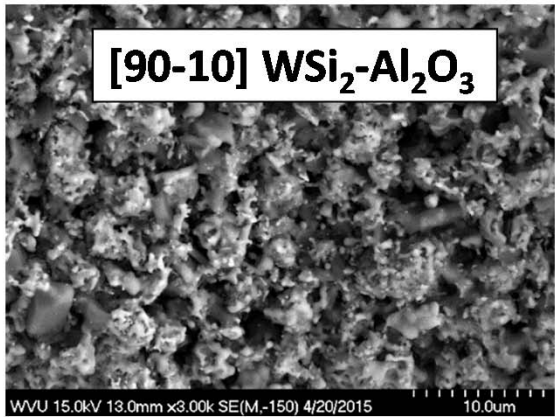

The SEM micrographs clearly shows that the thermocouples are fully dense and hence improves the conductivity

Image Analysis for Distribution (SEM):

Proposed Method: Determination of "coefficient of variation" as a measure of the degree of distribution (D index) by measuring distances between all neighboring silicide grains.

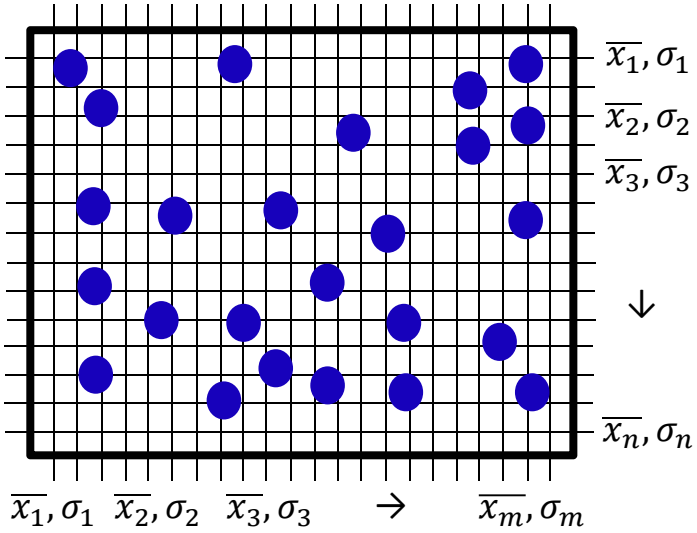

$$\bar{X} = \frac{(\overline{X_{h1}} + \overline{X_{h2}} + \cdots\cdots + \overline{X_{hN}}) + (\overline{X_{v1}} + \overline{X_{v2}} + \cdots\cdots + \overline{X_{vN}})}{2N}$$

$$s = \sqrt{\frac{[\sum_{i=1}^{N}(\overline{X_{hi}} - \bar{X})^2] + [\sum_{i=1}^{N}(\overline{X_{vi}} - \bar{X})^2]}{2N-1}}$$

$$D\ index = \left(\frac{s}{\bar{X}}\right)$$

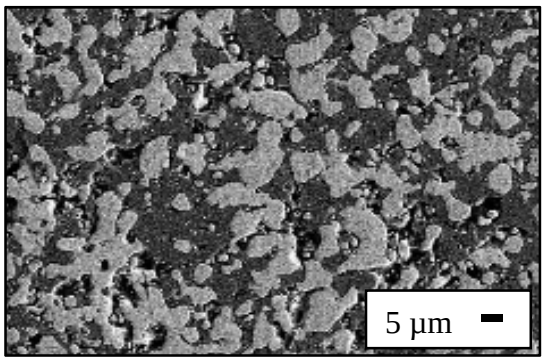

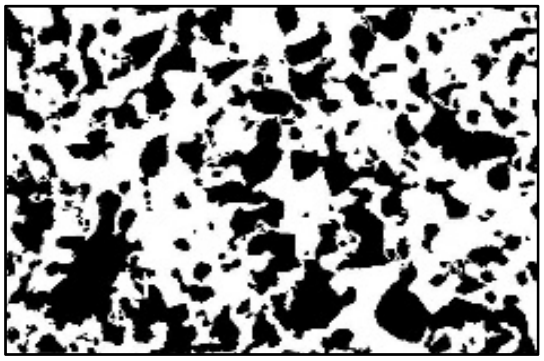

Original image → *Binary image*

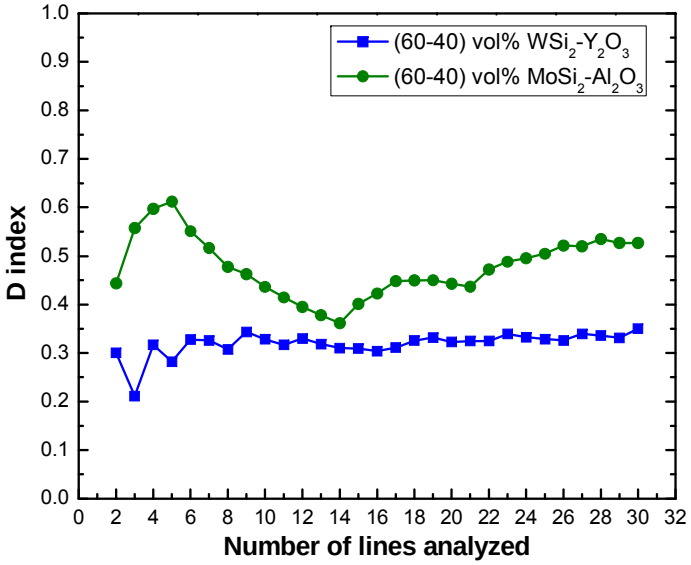

Silicide Thermocouples:

Thermoelectric Voltage

$$E_{AB} = \int_{T_2}^{T_1} \sigma_A(T)\,dT + \int_{T_1}^{T_2} \sigma_B(T)\,dT$$

Seebeck coefficients

Material	S_{500} (μV/°C)	Reference
$MoSi_2$	-3.0	T. Nonomura (2011)
WSi_2	-0.3	T. Nonomura (2011)
$TaSi_2$	14	Kenneth Kreider (1995)
$TiSi_2$	20.8	Kenneth Kreider (1995)
Pt	-3.3	Kenneth Kreider (1995)

Silicide Couples

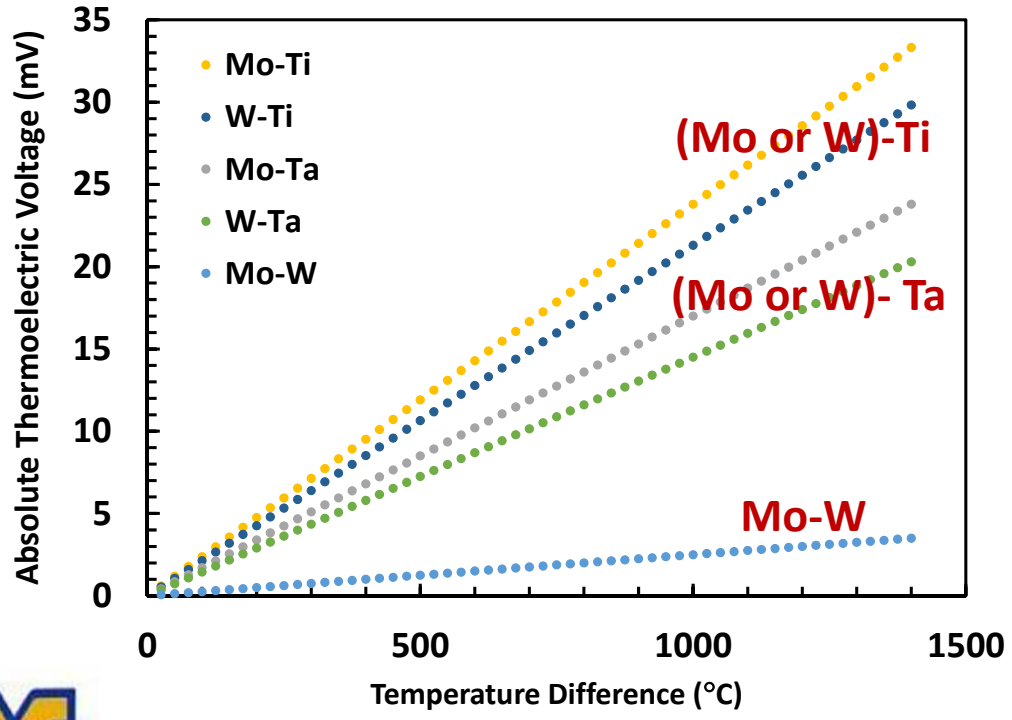

The emf generated between hot junction J_1 and cold junction J_2 in material A

- B-Type = 8.96 mV at 1400 °C
- (Mo or W)- Ti silicide couples ~ 30-34 mV at 1400 °C
- Mo-W silicide (most oxidation resistant) resulting only~ 4mV at 1400 ° C
- $CrSi_2$- based couples would perform nicely (σ = 200 μV/K) but melts at 1470 ° C

Embedded Thermocouple Preform:

Composite Powders

Dispersant (Solvents and Dispersants)

Organic Binder Vehicle

Ultrasonic mixing

Tape casted, laminated and laser cut alumina green substrates

Screen printing

Curing at 50 °C

Sintering at 1500 °C for 2 h. in Ar. atmosphere

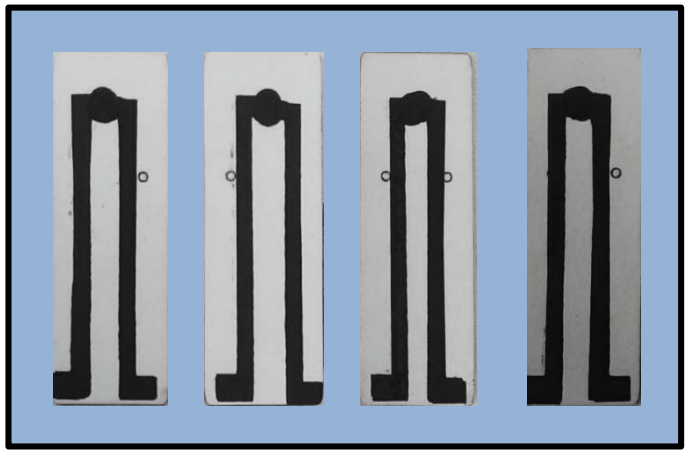

Ceramic Thermocouple Performance:

(High-temperature measurements)

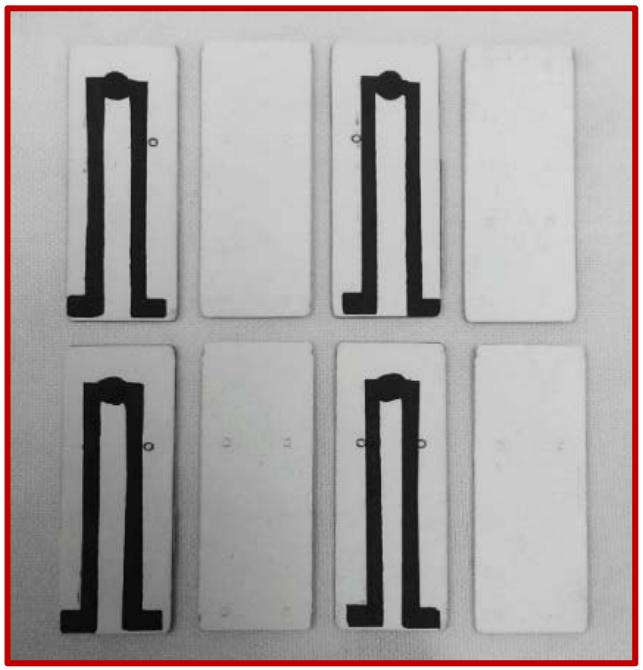

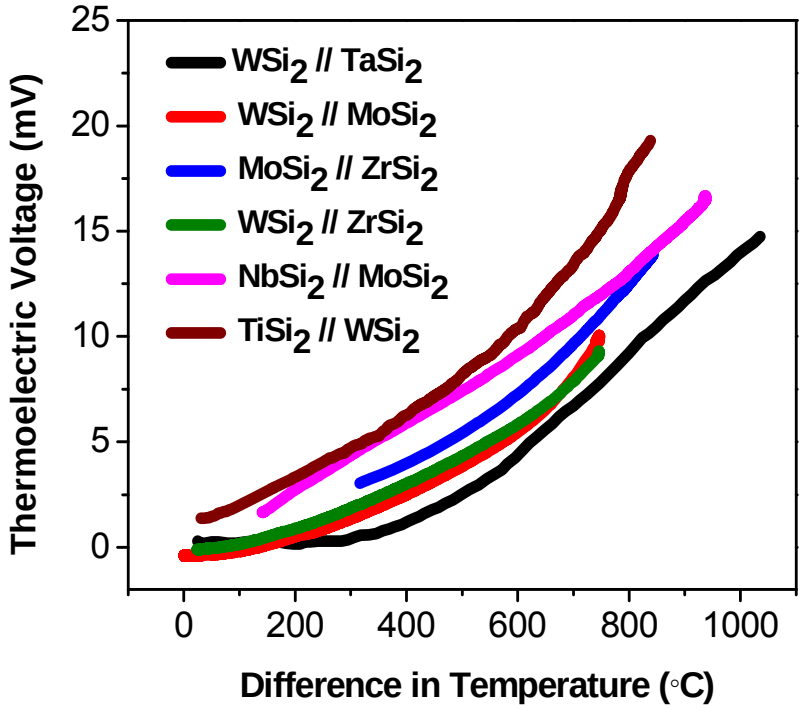

Preforms and laminated forms of ceramic thermocouples heated at 1500 °C and performance is evaluated at 1000 °C.

1. [90-10]WSi_2-Al_2O_3//[90-10]$TaSi_2$-Al_2O_3
2. [90-10WSi_2-Al_2O_3//[90-10] $MoSi_2$-Al_2O_3
3. [90-10]$MoSi_2$-Al_2O_3//[90-10] $ZrSi_2$-Al_2O_3
4. [90-10]WSi_2-Al_2O_3// [90-10] $ZrSi_2$-Al_2O_3
5. [90-10]$NbSi_2$-Al_2O_3//[90-10] $MoSi_2$-Al_2O_3
6. [90-10] $TiSi_2$-Al_2O_3//[90-10] WSi_2-Al_2O_3

$TiSi_2$// WSi_2 exhibited 20 mV at 800 °C

(Type B= 3.15 mV at 800°C)

Thermocouple Microstructures:

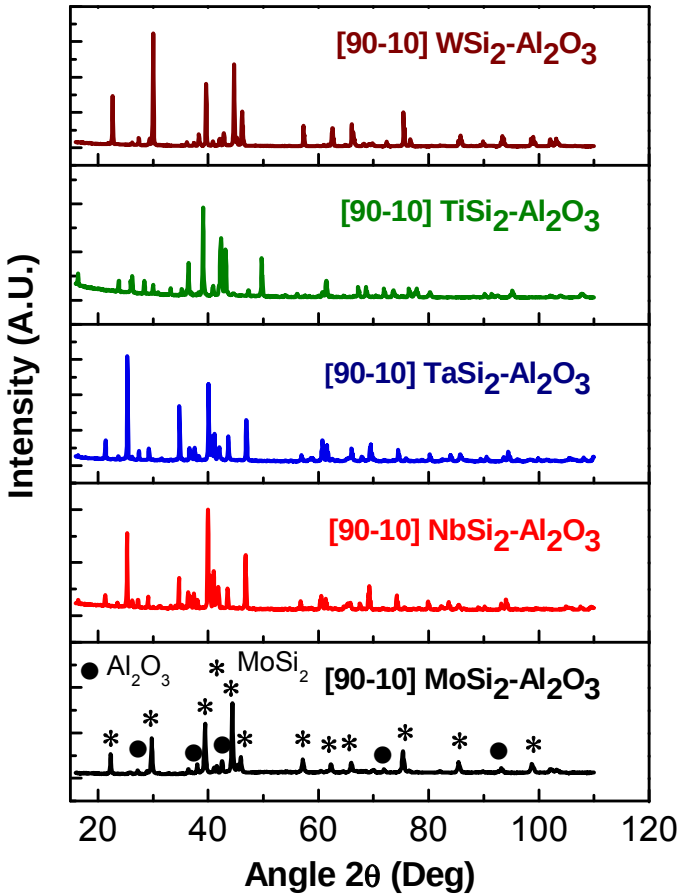

X-ray analysis of various ceramic-ceramic thermocouples sintered at 1500 °C in Ar

Ceramic Testing Stress/Strain Sensors:

- Introduce 10% oxygen flow into furnace during burnout of imbedded sensors to eliminate carbon deposits
- Texture substrates in the gripper area to prevent slipping during testing
- Amend sensor design to increase Gauge Factor
- Evaluate temperature effects on strain sensor
- Initiate compressive testing of ceramic strain sensors

Design ID	A	B	C
	(mm)	(mm)	(mm)
V3	40	1.0	1.0
V4	40	0.5	1.0
V5	40	0.5	0.5
V6	40	0.2	1.0
V7	40	0.2	0.5

A – Sensor length

B – Spacing between legs

C – Leg width

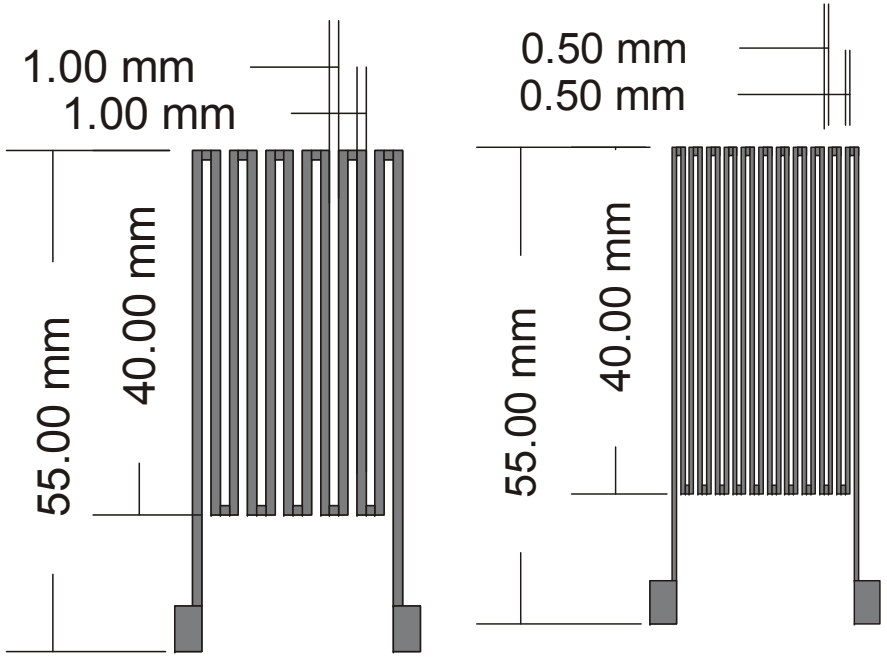

Design: V3 **Design: V5**

Embedded Thermocouple's Performance:

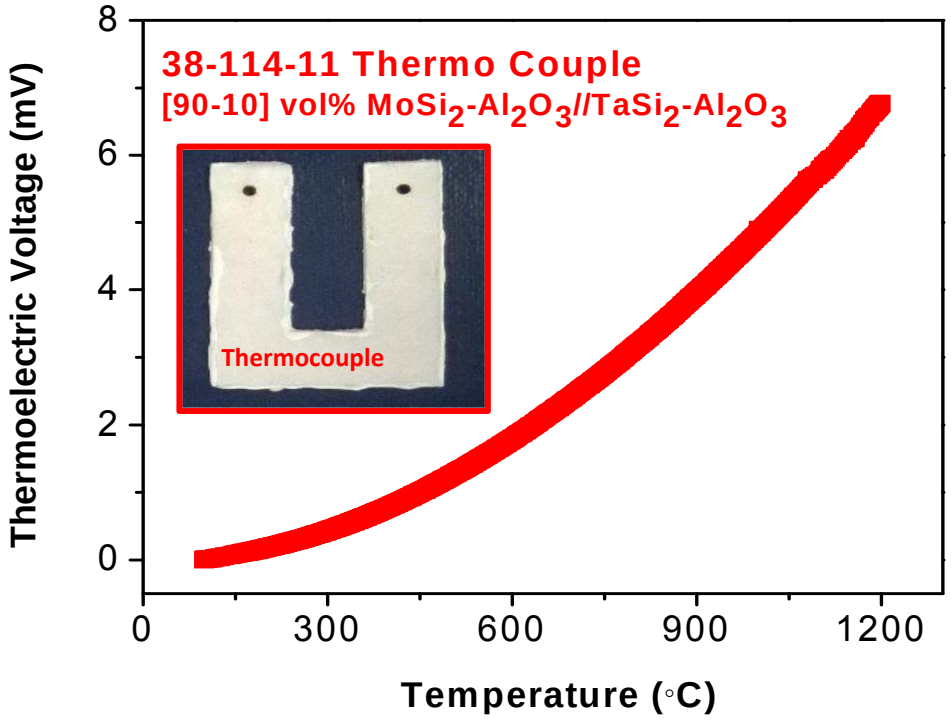

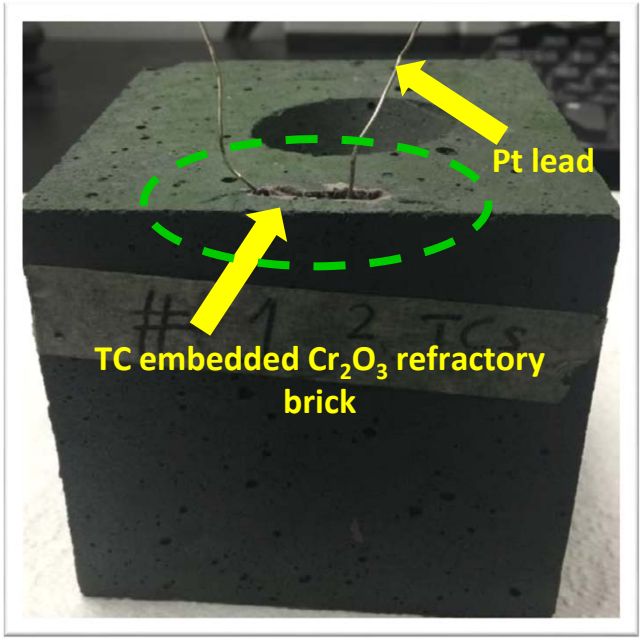

[90-10] vol% $MoSi_2$-Al_2O_3 // $TaSi_2$-Al_2O_3

- Thermocouple was embedded within the Cr_2O_3 refractory and was tested from room temperature to 1200 °C in argon atmosphere.
- Demonstrated half of predicted voltage, indicating some reaction or change in junction circuit.

Thermistor Preforms:

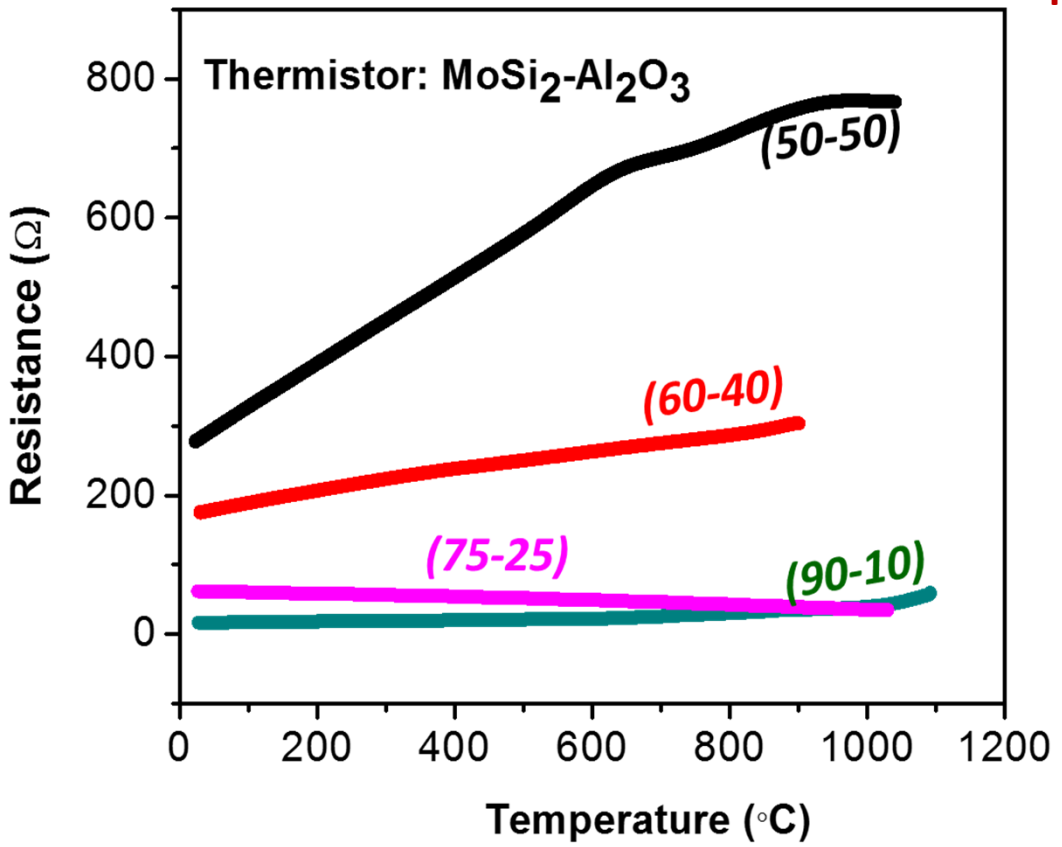

$MoSi_2$-Al_2O_3 based small thermistors

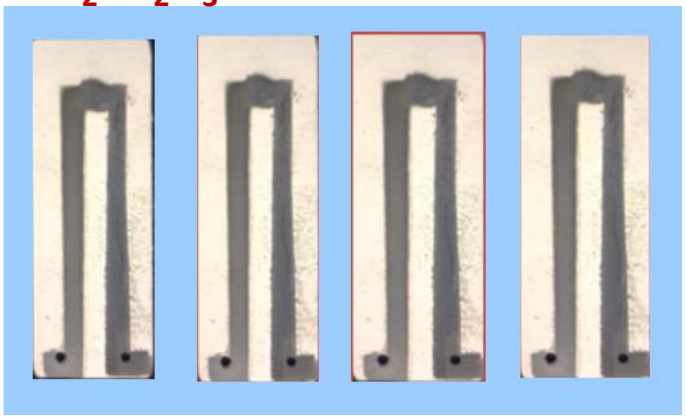

Sample ID	Temperature, °C	
Vol% of $MoSi_2$-Al_2O_3	100 °C	1000 °C
50-50	325.81	768.5
60-40	189.74	323.26
75-25	19.14	41.45
90-10	8.79	10.76

- Addition of $MoSi_2$ decreased the resistance of $MoSi_2$-Al_2O_3 composite thermistors [50-50] $MoSi_2$-Al_2O_3 exhibited 786.50 Ω and [90-10] $MoSi_2$-Al_2O_3 exhibited 10.76 Ω resistance at 1100 °C respectively

Static Cup Corrosion Study of Smart Brick:

Lab View Data

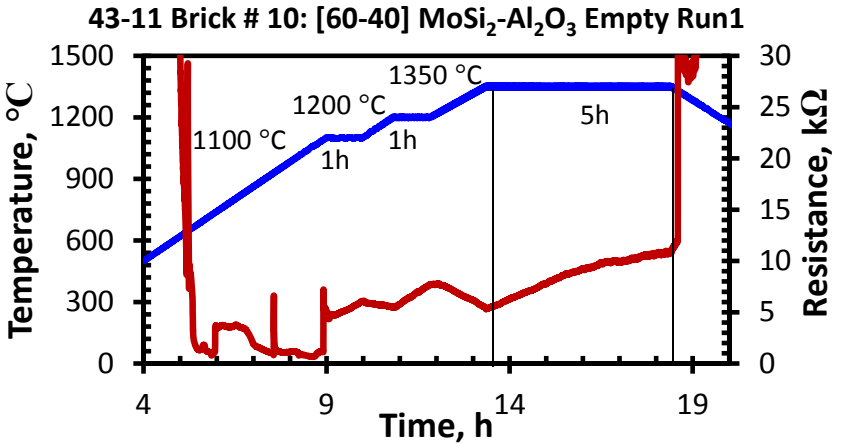

WSN Data

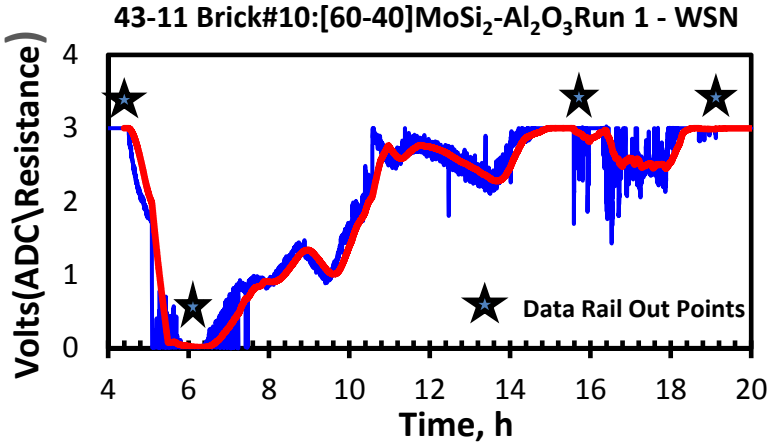

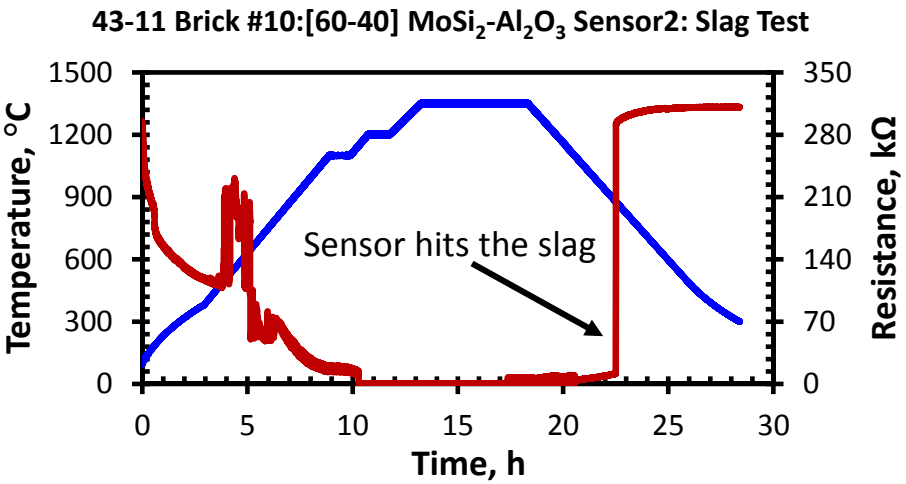

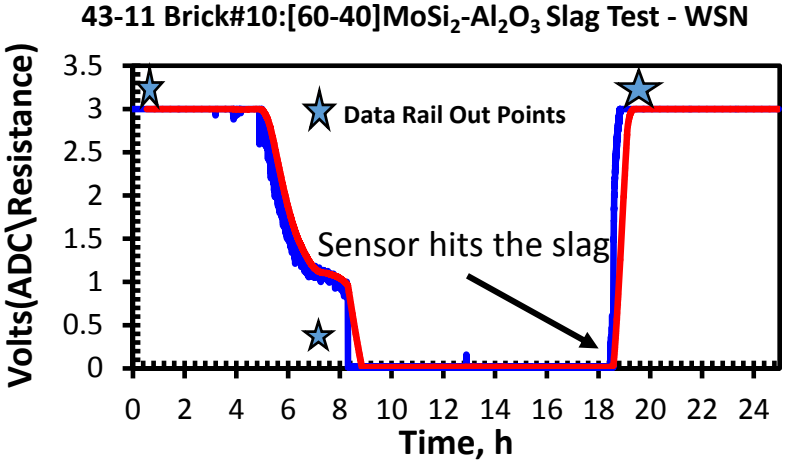

- The analytical test results (Lab View) of Brick #10: [60-40] $MoSi_2$-Al_2O_3 brick were correlated with wireless data up to 1350 °C isothermal hold and thereafter the data showed deviations. This may be due to oxidation.